The Plant Cell, Vol. 14, 2591–2612, October 2002, www.plantcell.org © 2002 American Society of Plant Biologists

Maize Opaque Endosperm Mutations Create Extensive Changes in Patterns of Gene Expression[W]

Brenda G. Hunter,[a] Mary K. Beatty,[b] George W. Singletary,[b] Bruce R. Hamaker,[c] Brian P. Dilkes,[a] Brian A. Larkins,[a] and Rudolf Jung[b,1]

[a] Department of Plant Sciences, University of Arizona, Tucson, Arizona 85721
[b] Pioneer Hi-Bred International, P.O. Box 1004, Johnston, Iowa 50131-1004
[c] Department of Food Science, Purdue University, West Lafayette, Indiana 47907

Maize starchy endosperm mutants have kernel phenotypes that include a brittle texture, susceptibility to insect pests, and inferior functional characteristics of products made from their flour. At least 18 such mutants have been identified, but only in the cases of *opaque2* (*o2*) and *floury2* (*fl2*), which affect different aspects of storage protein synthesis, is the molecular basis of the mutation known. To better understand the relationship between the phenotypes of these mutants and their biochemical bases, we characterized the protein and amino acid composition, as well as the mRNA transcript profiles, of nearly isogenic inbred lines of W64A *o1*, *o2*, *o5*, *o9*, *o11*, *Mucuronate* (*Mc*), *Defective endosperm B30* (*DeB30*), and *fl2*. The largest reductions in zein protein synthesis occur in the W64A *o2*, *DeB30*, and *fl2* mutants, which have ~35 to 55% of the wild-type level of storage proteins. Zeins in W64A *o5*, *o9*, *o11*, and *Mc* are within 80 to 90% of the amount found in the wild type. Only in the cases of *o5* and *Mc* were significant qualitative changes in zein synthesis observed. The pattern of gene expression in normal and mutant genotypes was assayed by profiling endosperm mRNA transcripts at 18 days after pollination with an Affymetrix GeneChip containing >1400 selected maize gene sequences. Compared with W64A *sugary1*, a mutant defective in starch synthesis, alterations in the gene expression patterns of the opaque mutants are very pleiotropic. Increased expression of genes associated with physiological stress, and the unfolded protein response, are common features of the opaque mutants. Based on global patterns of gene expression, these mutants were categorized in four phenotypic groups as follows: W64A+ and *o1*; *o2*; *o5*/*o9*/*o11*; and *Mc* and *fl2*.

INTRODUCTION

Endosperm texture is an important quality trait in maize, because it influences the shipping and handling characteristics of the grain, the susceptibility to insect pests, the yield of grits from dry milling, energy costs during wet milling, and the baking properties of the flour. The genetic, biochemical, and environmental factors that contribute to texture (i.e., hardness and vitreousness) are poorly understood (Chandrashekar and Mazhar, 1999). Kernel texture is related at least partially to the formation of a vitreous, or glassy, endosperm, and this is influenced by the protein content of the seed and the conditions of the kernel during maturation and desiccation (Kirleis and Stroshine, 1990; Mestres and Matencio, 1996). There appears to be a relationship between kernel hardness and storage protein synthesis in the endosperm, because factors that influence storage protein accumulation, such as nitrogen fertilization (Tsai et al., 1978) and deposition in protein bodies during endosperm development, are related to kernel phenotype (Coleman and Larkins, 1999).

The major storage proteins in maize endosperm are a group of prolamins known as zeins. Zeins are synthesized on rough endoplasmic reticulum (ER) membranes and accumulate in the ER as insoluble accretions called protein bodies (Larkins and Hurkman, 1978). There are three structurally distinct types of zein proteins, and they are distributed asymmetrically in protein bodies (Lending and Larkins, 1989; Woo et al., 2001). Mutations that alter zein synthesis can lead to protein bodies with abnormal morphology, size, or number, and they result in kernels with a soft, starchy texture. Mutations that reduce α-zein synthesis, such as *opaque2* (*o2*), result in small, unexpanded protein bodies (Geetha et al., 1991), whereas those that reduce γ-zein synthesis, such as *o15* (Dannenhoffer et al., 1995), lead to a smaller number of protein bodies. Conversely, the overproduction of γ-zein appears to enhance protein body number and result in the formation of more vitreous endosperm (Lopes et al., 1995; Moro et al., 1995). Other opaque mutants, such as *floury2* (*fl2*), *Mucuronate* (*Mc*), and *Defective*

[1] To whom correspondence should be addressed. E-mail rudolf.jung@pioneer.com; fax 515-254-2619.
[W] Online version contains Web-only data.
Article, publication date, and citation information can be found at www.plantcell.org/cgi/doi/10.1105/tpc.003905.

endosperm B30 (*DeB30*), are associated with irregularly shaped protein bodies (Fontes et al., 1991; Coleman et al., 1997b). However, it is not clear whether the apparent link between a starchy endosperm phenotype and the synthesis and deposition of zeins is the result of a causal relationship or whether both are secondary, perhaps pleiotropic, effects of the mutations. For example, the *o1* mutation appears to have little effect on zein synthesis (Nelson et al., 1965), yet it results in a soft, starchy endosperm. Furthermore, an opaque phenotype also has been observed as a result of nutritional, mechanical, and biotic stresses, and it is common among *dek* mutants (Lyznik and Tsai, 1989; Neuffer et al., 1997; O.A. Olsen, personal communication).

At least 18 mutations have been described that cause a soft, starchy endosperm phenotype (Thompson and Larkins, 1994). Only in the case of *o2* and *fl2* is the molecular basis for the mutation understood. *o2* encodes a transcription factor that regulates genes encoding the 22-kD α-zeins as well as several other proteins (Damerval and De Vienne, 1993; Habben et al., 1993). *fl2* corresponds to a point mutation in the signal peptide of a 22-kD α-zein protein (Coleman et al., 1997b). Failure to correctly process this signal peptide appears to cause the protein to become anchored to the ER membrane, leading to the creation of foci of hydrophobic α-zeins at the surfaces of protein bodies (Gillikin et al., 1997). This results in a dramatic increase in the synthesis of binding protein and other ER-resident chaperones, indicating an unfolded protein response in endosperm cells (Fontes et al., 1991; Coleman et al., 1997b; Shank et al., 2001). Biochemical responses in some opaque mutants appear similar to those in *o2* and *fl2*. For instance, in endosperm of *Mc* and *DeB30*, ER-resident chaperones are induced dramatically (Zhang and Boston, 1992; Shank et al., 2001). However, a direct comparison of the various opaque mutants has been difficult because of their occurrence in different genetic backgrounds and the variation in penetrance of the mutant phenotype in these backgrounds (Balconi et al., 1998).

To better understand the nature of the mutations associated with a starchy endosperm phenotype, we developed nearly isogenic lines of a number of opaque mutants and compared their effects on protein synthesis and amino acid composition. We also compared the pattern of gene expression in these mutants by transcript profiling with Affymetrix GeneChip arrays. Our results reveal distinct, as well as shared, gene expression patterns in these mutants, and they provide a framework for investigating a common mechanism that underlies the opaque kernel phenotype.

RESULTS

To systematically compare the protein composition and patterns of gene expression between opaque mutants, we backcrossed the *o1*, *o5*, *o9*, *o11*, *DeB30*, and *Mc* mutations into the W64A inbred line. After six generations of backcrossing and two generations of self-pollination, each of the inbred lines appeared to be homogeneous, resembling the recurrent parent with respect to plant height, color, and tassel morphology and resembling the mutant with respect to an opaque endosperm phenotype. The independently developed nearly isogenic lines of W64A *sugary1* (*su1*), *fl2*, and *o2* (see Methods) were phenotypically consistent with these lines. The *o5* and *o9* plants tended to have yellow seedlings at the two- to four-leaf stage, although they greened as the plants developed. The yellow phenotype of *o5* agrees with a previous description of this mutant (Neuffer et al., 1997). In addition, *o5* and *o9* developed more slowly than the wild-type and mutant inbred lines. *o5* typically flowered 1 week later, whereas flowering in *o9* usually was delayed by 10 to 14 days.

We measured the protein and amino acid contents of the endosperm from these mutants to determine if they manifested large qualitative or quantitative differences in zein and nonzein protein composition compared with the wild type (Table 1). This analysis demonstrated a significant degree of similarity among the inbred lines: the wild type and *o1*, *o9*, *o11*, and *DeB30* mutants each contained ~12% protein, whereas the *o5*, *Mc*, and *fl2* mutants were very close to this value (i.e., 11.5 to 11.8% protein). The *o2* mutant contained 10.1% protein; this amounts to a reduction in total protein of ~15%. There was variability among the mutants with regard to the partitioning of proteins between the zein and nonzein fractions. The amount of nonzein protein in *o1* and *o5* was nearly identical to that in the wild type (2.1 mg/100 mg dry weight). The largest increases in nonzein proteins were in *o2*, *o11*, *DeB30*, and *fl2*, which contained ~70% more protein than the wild type. Nonprotein nitrogen was most increased in *o2*, which is consistent with the high level of free amino acids in this mutant (Wang and Larkins, 2001). The amount of nonprotein nitrogen in *o1* was similar to that in the wild type, whereas that in most of the other mutants was intermediate between the wild type and *o2*.

With the exception of *o1*, each of the mutants had a higher Lys content than the wild type, but there were three distinct levels of increase: *o2* had more than twice the amount in the wild type; *o11*, *DeB30*, and *fl2* had 1.8 times the amount in the wild type; and *o5*, *o9*, and *Mc* had 1.4 times the amount in the wild type. A similar pattern was observed with respect to increases in Arg and Asn/Asp content. Among the amino acids reduced in the opaque mutants, except *o1*, were Gln/Glu, Leu, and Pro, the most abundant amino acids in zein proteins. The reduction of these amino acids generally was reciprocal to the increase in Lys.

SDS-PAGE was used to compare qualitative and, to some degree, quantitative differences in specific proteins among the opaque mutants. To standardize these comparisons, proteins from equal weights of endosperm flour of each genotype were extracted and partitioned into zein and nonzein fractions (Wallace et al., 1990). Figure 1A shows a Coomassie blue–stained gel showing the total zein fraction ob-

Table 1. Protein and Amino Acid Composition of Mature Endosperm of W64A+ and Selected Opaque Mutants

Protein/Amino Acid	Wild Type (%)	*o1* (%)	*o2* (%)	*o5* (%)	*o9* (%)	*o11* (%)	*Mc* (%)	*DeB30* (%)	*fl2* (%)
Total protein	12.1	12.8	10.1	11.5	12.2	12.0	11.7	12.0	11.8
Zein protein	8.2	8.5	2.9	6.4	7.3	6.4	7.2	4.5	5.9
Nonzein protein	2.1	2.1	3.6	2.0	2.8	3.4	2.7	3.8	3.7
Nonprotein nitrogen	0.6	0.7	2.3	1.5	1.3	1.4	1.4	1.7	0.9
Cys	1.8	1.8	2.4	2.0	1.8	1.9	1.6	2.0	1.9
Asx	6.6	7.2	13.2	7.7	7.5	8.6	8.0	9.8	8.4
Met	2.7	2.8	2.5	3.0	2.6	2.9	3.1	3.0	3.5
Thr	3.4	3.5	3.8	3.7	3.5	3.8	3.6	3.9	3.8
Ser	5.4	5.6	5.2	5.5	5.6	5.3	5.5	5.4	5.4
Glx	23.2	22.6	19.5	21.6	22.4	20.5	22.0	20.8	20.3
Pro	9.4	9.0	7.4	9.1	9.0	8.5	8.5	8.3	8.0
Gly	2.3	2.5	3.8	2.9	2.7	3.2	2.6	3.1	3.1
Ala	8.3	8.2	6.4	7.9	8.1	7.7	8.1	7.3	7.8
Val	5.1	5.2	5.8	5.3	5.2	5.9	5.3	5.7	5.5
Ile	3.7	3.7	3.5	3.7	3.6	3.8	3.8	3.6	3.8
Leu	15.0	14.6	8.7	13.6	13.8	12.5	14.1	11.6	12.9
Phe	5.4	5.5	4.4	5.2	5.2	5.0	5.3	4.9	5.3
His	2.3	2.3	2.9	2.4	2.2	2.5	2.2	2.4	2.3
Lys	1.5	1.7	3.8	2.1	2.0	2.8	2.1	2.9	2.8
Arg	3.8	4.0	6.7	4.3	4.7	5.1	4.2	5.3	5.2

Protein and nonprotein nitrogen compositions are given in percent dry weight. Amino acid compositions are given in percent protein (w/w).

tained from the wild-type and opaque mutant inbred lines. With the exception of *o2*, which showed the characteristic reduction in 22-kD α-zeins (Lee et al., 1976), there were no obvious differences in the major zein components detected among these mutants. However, in Coomassie blue–stained gels, the less abundant zein proteins are not always identified easily (Woo et al., 2001), and the very abundant 22- and 19-kD α-zeins can interfere with the detection of similarly sized zein proteins (i.e., the 18-kD δ-, 16-kD γ-, and 15-kD β-zeins). Therefore, the proteins also were identified by immunodetection.

Immunoblotting with 50-kD (Figure 1B) and 27-kD (Figure 1C) γ-zein–specific antisera showed no differences in the sizes and no reproducible differences in the amounts of these proteins in wild-type and opaque mutant endosperms. With the exception of *Mc*, reaction with the 16-kD γ-zein antiserum also showed no differences in protein patterns (Figure 1D). Two weakly stained polypeptides were detected in *Mc*. One migrated at 16 kD, and the second migrated with an apparent molecular mass of 13 kD. A reduction of the signal detected with the 15-kD β-zein–specific antiserum was seen in *o2* (Figure 1E).

Antiserum recognizing total α-zeins from W64A (Lending et al., 1988) detected differences in the proteins in *o2* and *fl2* but not in the other opaque mutants. There was a marked reduction in 22-kD α-zeins in *o2*; *fl2* also showed a reduction in 22-kD α-zeins, as well as a mutant α-zein, the 24-kD *fl2* gene product (Figure 1F, arrow) (Coleman et al., 1997b). Similar differences were observed with a 22-kD α-zein–specific antibody (Figure 1G); however, the 24-kD *fl2* α-zein was not detected readily on this immunoblot. In addition to reaction with a major band at 19 kD, the 19-kD Bα-zein antiserum reacted with a slightly larger polypeptide in the normal and mutant genotypes (Figure 1H). This larger protein is most likely the product of the 19-kD B-2 α-zein gene, which has a 33–amino acid insertion (Woo et al., 2001). The pattern of immunostaining among the different opaque mutants was fundamentally similar, except in *fl2*, which had an additional, even slower migrating polypeptide. This is most likely a modified α-zein, as noted previously for this mutant (Lopes et al., 1994). Immunoreaction with the 19-kD Dα-zein antiserum revealed no obvious differences in proteins among the normal and mutant backgrounds (Figure 1I).

To specifically detect the 18-kD δ-zein, blots were probed first with an antibody that was raised against a 25-residue peptide derived from the B73 allele of 18-kD δ-zein (Woo et al., 2001). However, no signal was detected in any of the zein extracts (data not shown). Because the 18-kD δ-zein was found to show considerable allelic variation, the blots were probed with a different antibody (see Methods) that recognizes a wide spectrum of 18-kD δ-zein alleles (R. Jung, unpublished data). With the notable exception of *o5*, we did not detect 18-kD δ-zein–specific bands in W64A+ and in the nearly isogenic mutant lines with this antibody (Figure 1J). In *o5*, the blot showed a number of strong, but poorly resolved, bands. Some of these are larger than 18 kD, and it was not clear whether this is the result of a distortion (masking) because of coincident electrophoretic mobility of the very abundant α-zein polypeptides. In extracts from each of the inbred lines, the 18-kD δ-zein antibody cross-reacted

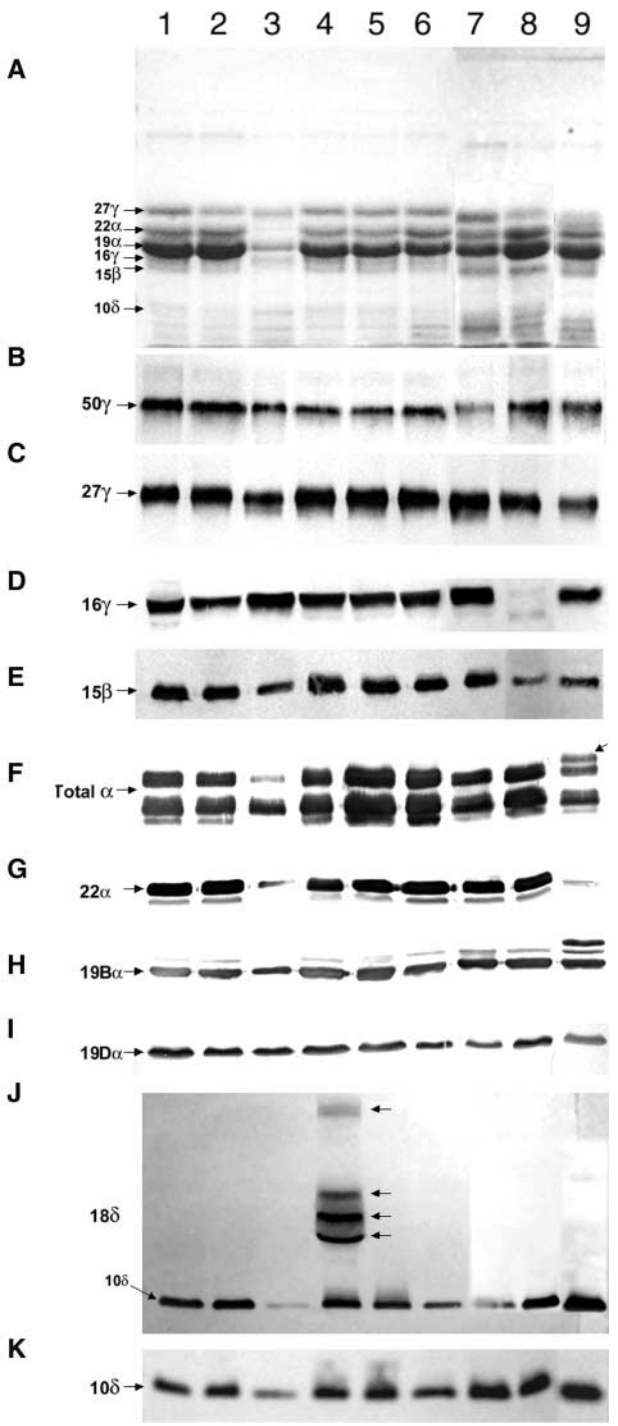

Figure 1. SDS-PAGE Analysis of Zein Proteins in the Wild Type and Opaque Endosperm Mutants.

(A) Coomassie blue–stained 12.5% polyacrylamide gel showing total zeins extracted from 750 μg of endosperm flour. Lane 1, W64A+; lane 2, *o1*; lane 3, *o2*; lane 4, *o5*; lane 5, *o9*; lane 6, *o11*; lane 7, *DeB30*; lane 8, *Mc*; lane 9, *fl2*.

with a 10-kD peptide, probably the 10-kD δ-zein, and a reduction of the 10-kD signal was seen in *o2* (Figure 1J). The monospecific 10-kD δ-zein antiserum (Figure 1K) reacted similarly with protein from the wild type and the opaque mutants. In *o2*, there was again a notable reduction in the 10-kD δ-zein signal, as was the case with the 18-kD δ-zein antibody.

Figure 2A shows a Coomassie blue–stained polyacrylamide gel from SDS-PAGE separation of the nonzein protein extracts of W64A+ and the different opaque mutants. The protein in these samples was based on equal weights of endosperm flour, and the greater staining intensity in lanes 3, 7, and 9 reflects the increased amount of nonzein proteins in *o2*, *DeB30*, and *fl2*, respectively (Table 1). Recently, several novel globulin proteins—18-kD α-globulin, legumin1, and legumin2—were detected in maize endosperm (Woo et al., 2001; R. Jung, unpublished data). During extraction, these globulin proteins partition into the nonzein fraction (Wallace et al., 1990). We did not detect any qualitative or quantitative differences in the level of legumin1 or legumin2 in the wild-type and mutant inbred lines (Figures 2B and 2C, respectively). The anti-globulin antiserum revealed slight differences in the amount of this protein among some of the opaque mutants, and it routinely had a slightly slower migration in *o5*, suggesting altered processing or an allele that encodes a protein with a slightly larger molecular mass (Figure 2D).

GeneChip Microarray Analysis of Maize Endosperm mRNA Transcripts

Endosperm mRNAs in W64A+ and the nearly isogenic opaque mutants were analyzed using a GeneChip microarray produced by Affymetrix. The GeneChip contained arrays corresponding to >1400 maize genes selected from the Pioneer Hi-Bred EST database (see supplemental data online), and sequences corresponding to the majority of these genes (or their alleles/gene family members) also were identified in endosperm cDNA libraries. The transcript level in developing B73 endosperm for several genes in this array was described previously (Woo et al., 2001).

Duplicate GeneChip microarrays were hybridized with copy RNA (cRNA) targets from two replicated kernel sam-

(B) to **(K)** Immunoblots developed with antisera against the 50-kD γ-zein **(B)**, 27-kD γ-zein **(C)**, 16-kD γ-zein **(D)**, 15-kD β-zein **(E)**, total α-zein **(F)**, 22-kD α-zein **(G)**, 19-kD Bα-zein **(H)**, 19-kD Dα-zein **(I)**, 18-kD δ-zein **(J)**, and 10-kD δ-zein **(K)**. Protein samples in **(B)** and **(C)** were extracted from 15 μg of flour, whereas the others were extracted from 75 μg of flour. The antisera concentrations are described in Methods.

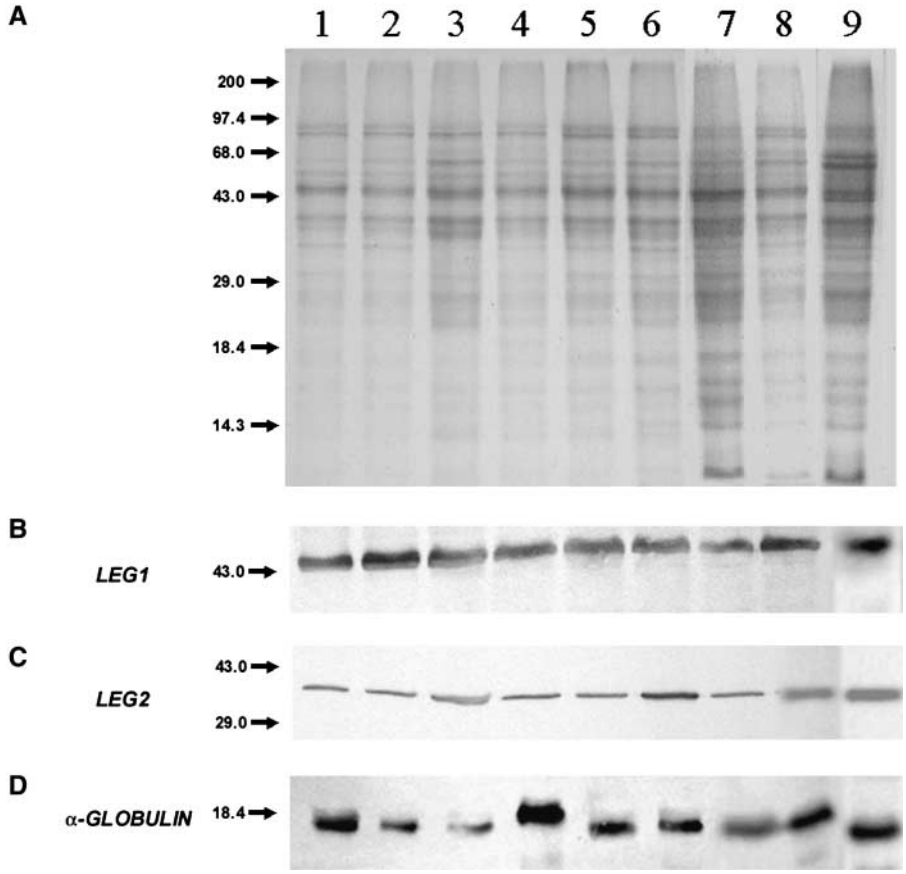

Figure 2. SDS-PAGE Analysis of Nonzein Seed Proteins in the Wild Type and Opaque Endosperm Mutants.

(A) Coomassie blue–stained 12.5% polyacrylamide gel showing total nonzein proteins extracted from 1.5 mg of flour. Lane 1, W64A+; lane 2, *o1*; lane 3, *o2*; lane 4, *o5*; lane 5, *o9*; lane 6, *o11*; lane 7, *DeB30*; lane 8, *Mc*; lane 9, *fl2*.
(B) to **(D)** Immunoblots developed with antisera against legumin1 **(B)**, legumin2 **(C)**, and α-globulin **(D)**. Protein was from 750 μg of flour. The antisera concentrations are described in Methods.

ples (see Methods). In typical experiments, each sample was prepared from endosperm tissue pooled from three ears to minimize the effect of biological variation. Because of the expense of the Affymetrix GeneChip, hybridization experiments with cRNA from each replica sample were conducted only once. The experimental conditions, including demonstration of deoxyribonucleotide probe excess, were optimized independently and demonstrated to provide highly reproducible results (M.K. Beatty, unpublished data).

The results obtained after hybridization of the GeneChip with cRNAs revealed a strong pleiotropic effect of the opaque mutations on gene expression. This result made the transcript data refractory to the normalization procedure recommended by Affymetrix (Wodicka et al., 1997). Therefore, to allow a direct comparison of the transcript data set from each genotype, successive regression analyses (see Methods) were used to normalize these data and to globally scale them to that of W64A+. This procedure generated scaled values for each gene and permitted a direct comparison of all data points, regardless of the experiment from which they originated. This resulted in normalized GeneChip intensities that varied in their cumulative values of expression intensity for the different mutants (Table 2). For example, the normalized cumulative expression intensity of W64A *o2* arrays (121,365) was approximately one-third lower than that of W64A+ (176,300), perhaps as a direct result of the downregulation of highly expressed zein genes (Lee et al., 1976). The cumulative expression intensity of W64A *o11* (268,500) was approximately one-third larger than that of W64A+, indicating increased expression of many genes (see below).

Table 2. Maize GeneChip Ranges of Normalized Expression Intensities

Experiment	*OH43+*	*W64A+*	*su1*	*o1*	*o2*	*o5*	*o9*	*o11*	*Mc*	*fl2*
Cumulative normalized expression intensity of chip	186,852.1	176,277.7	190,553.2	192,550	121,364.9	191,785.6	232,239	268,544	237,847.6	172,352.1
Genes total	1,488	1,488	1,488	1,488	1,488	1,488	1,488	1,488	1,488	1,488
Genes with negative expression intensity[a]	299	301	252	330	551	318	385	300	337	337
Genes with expression intensity <20 (arbitrary baseline)	873	977	830	796	875	756	721	717	765	885
Genes with expression intensity >20	615	512	658	692	613	732	767	771	723	603
Genes with expression intensity >0.1% of cumulative chip intensity	195	135	123	148	266	194	183	188	168	159
Genes with expression intensity >1% of cumulative chip intensity	25	21	19	22	25	19	23	23	28	26

[a] Average hybridization signal of matched oligodeoxyribonucleotide probe set < average hybridization signal of mismatch probe set.

In each analysis, ~20% of the genes had negative expression intensities (Table 2), indicating that the matched oligodeoxyribonucleotide probe set had a lower hybridization signal than the mismatched set of probes. These negative values were reproducible within genotypes and did not result from a failure in hybridization or scanning. This result could be explained by the presence of nearly identical transcripts (alleles) with higher expression levels than the probe gene that hybridized to the mismatched set of probes. Reasons for the strong hybridization signals in the mismatch set are difficult to evaluate, because Affymetrix does not disclose the oligodeoxyribonucleotide sequences of matched and mismatched probes. However, in a few cases, oligodeoxyribonucleotide sequences were provided, and comparison of these sequences with those in public and proprietary databases by BLAST analysis supported the hypothesis that allelism is a major cause of the negative expression values (data not shown). Because of these ambiguities, expression values of <20, including negative values, were considered "not detected" and, according to Affymetrix conventions, were systematically set to 20 arbitrary expression units (baseline). Consequently, the expression of between 500 and 700 genes on the GeneChip was regarded to be at baseline and therefore not interpretable in any of the endosperm transcript profiling experiments. This reflects the presence of many genes on the microarray for which expression is below the detection limit or that are not expressed in endosperm tissue. Interestingly, the number of expressed genes detected in the mutants was 10 to 15% greater than that in the wild type. Approximately 10% of the genes on the microarray were expressed at >0.1% of the cumulative expression intensity, and ~1.5% of the genes were expressed at >1% of the cumulative expression intensity. In W64A+, the latter consisted of mostly seed storage protein transcripts, whereas in the mutants, they also included other types of mRNAs (see below). This result reflects the abundance of a given mRNA relative to its concentration in each of the total mRNA populations. The results with *o2* stand out among these measurements, because the expression of 266 genes was >0.1% of the cumulative expression intensity, which is twice the number measured in the wild type (135 genes).

Table 3 shows a subset of the expression data (the entire data set is presented in the supplemental data online). It is easily recognized that endosperm storage protein genes had the highest levels of transcripts. The relative expression intensities in W64A+ for the 19-kD Bα-zein genes (Table 3, rows 153 to 155) and the 22-kD α-zein genes (Table 3, rows 149, 150, 156, and 157) were in the range of 5000 and 10,000 arbitrary expression units. The cumulative intensity of the array analysis for W64A+ was ~175,000 arbitrary expression units; therefore, provided that expression units and transcript abundance are related linearly, each of the α-zein genes apparently accounted for ~2.5 to 5% of the total transcript population. These data are consistent with our previous estimates of transcripts for the corresponding genes in W64A+ (Marks et al., 1985) and B73 endosperm (Woo et al., 2001). Similarly, in accordance with the literature (Kodrzycki et al., 1989; Lohmer et al., 1991), in W64A *o2*, the GeneChip expression intensities of the 22-kD α-zein genes and the gene encoding the ribosome-inactivating protein (Table 3, row 222) were diminished between 200- and 3-fold, respectively, compared with that of W64A+.

The α-zeins, as well as other zein genes on the GeneChip, are members of closely related multigene families, but the results demonstrate that the expression of these genes can be evaluated independently. For example, the expression intensities of the 22-kD α-zein Z1 gene were 4823, 20, and 2650 in W64A+, W64A *o2*, and W64A *o5*, respectively (Table 3, row 149). Expression intensities of the 22-kD α-zein Z5 gene, which is 93% identical to the Z1 gene, were 5756, 20, and 20 in W64A+, W64A *o2*, and W64A *o5*, respectively

(Table 3, row 150). The fact that the expression of these two nearly identical genes was detected differentially (i.e., different intensity levels are detected in *o2* compared with *o5*) validates the utility of the GeneChip assay for endosperm mRNA transcript profiling.

Comparison of Endosperm mRNA Transcripts in W64A+, W64A *su1*, and the Nearly Isogenic Opaque Mutants

Eighteen to 22 days after pollination (DAP) endosperm was chosen for comparison of mRNA transcripts between genotypes, because by this stage the majority of cells have ceased division and take on a mature differentiation state, reflecting a high level of starch and storage protein synthesis. Furthermore, high-quality RNA can be prepared from endosperm at this period of development. Several control experiments were performed to assess biological variation in gene expression as a result of ear sampling and the potential differences in gene expression measurements that result simply from allelic variation. Figure 3A shows a scatterplot analysis comparing transcripts in two different ears of 22 DAP W64A+. The regression analysis of these data yielded a very high coefficient of determination ($R^2 = 0.996$), indicating nearly genetic identity between the samples and a high degree of reproducibility in the Affymetrix analysis of the transcripts. These data were replotted in Figure 3B, which shows an expanded view of the genes with expression intensities between 20 and 1000. The small degree of scatter among these data further illustrates the similarity in the level of gene expression between the two samples. Because the latter presentation provided a significant degree of resolution for most of the expressed genes on the microarray, it was used routinely to globally compare transcript data sets.

Figure 3C shows a similar type of comparison with RNA transcripts from 18-DAP endosperm of W64A+ and Oh43+. In this case, the coefficient of determination is 0.862, indicating a much greater degree of variability in signal intensity than was observed in the W64A+ comparison described above. The variability in these samples is much more apparent in the presentation of the data in Figure 3D, which shows the expanded view of genes with expression intensities between 20 and 1000. Regression analysis of the data from the Oh43 replicates yielded a higher coefficient of determination ($R^2 = 0.99$), demonstrating that the differences between W64A and Oh43 cannot be accounted for by a greater variance between the Oh43 replicates. This variability in transcript profiling most likely is a consequence of allelic variation between inbred lines and indicates the importance of using nearly isogenic lines to compare variability in gene expression among the mutants.

Figure 3E presents a comparison of mRNA transcripts in 18-DAP W64A+ and W64A *su1*. *su1* encodes a starch-debranching enzyme (isoamylase), and the *su1-1* mutant leads to increased Suc concentration, decreased amylopectin content, and a collapsed endosperm phenotype at maturity as a result of the synthesis of water-soluble phytoglycogen (James et al., 1995). Comparison of mRNA transcripts in 18-DAP endosperm of the wild-type and *su1* endosperms revealed very few differences in gene expression, in spite of the severity of the kernel phenotype at maturity. Although *su1* is considered a pleiotropic mutant (Giroux et al., 1994), the linear regression analysis of these data produced a coefficient of determination ($R^2 = 0.998$) that is as high as that produced by the comparison between the two wild-type ears (cf. Figures 3A and 3E). Only 21 genes were found to have an expression level that is at least twofold greater than that of the wild type, and the expression of no gene was $<$50% that of the wild type (Table 3). Most of the genes that showed an increased level of expression, such as molecular chaperones and wound-induced and Hyp-rich proteins, are related to stress responses. The transcript level of *su1*, like that of other genes encoding starch biosynthetic enzymes, was not altered in this mutant, in agreement with the finding of James et al. (1995) for the reference allele (*su1*-ref) used in this study.

The *o2* gene has a much greater impact than *su1* on gene expression in 18-DAP endosperm. As shown in Figure 3F, the expression of a large number of genes was different from that of the wild type, as reflected by the coefficient of determination ($R^2 = 0.71$) in the scatterplot. Sixty genes were upregulated more than threefold relative to the wild type, and these accounted for ~15% of the total gene expression intensity measured by the microarray (see supplemental data online). These genes appear to function in a number of pathways, although it was difficult to extrapolate a unifying explanation. However, 19 upregulated genes belong to the complex of genes related to stress responses, molecular chaperones, and protein turnover. Transcripts for genes encoding ubiquinol–cytochrome *c* reductase, glutathione *S*-transferase, β-glucosidase, and a zeamatin-like protein each accounted for >1% of the cumulative gene expression intensity on the chip. The expression of 66 genes was reduced more than threefold compared with that of the wild type. Among these are genes encoding zein storage proteins (all 22-kD α-zeins, one 19-kD Dα-zein, 15-kD β-zein, and 10-kD δ-zein), ribosome-inactivating protein (RIP), aldolase, enolase, orthophosphate dikinase, actin, and α-tubulin. In contrast to zein proteins, transcripts of two nonzein seed proteins that typically are expressed preferentially in the embryo (germin-like protein and globulin1) were increased. The transcript of the *o2* gene was reduced fivefold. Notably, many of the downregulated genes are involved in carbon metabolism and carbohydrate metabolism. Some genes putatively involved in amino acid metabolism were upregulated (e.g., Ser *o*-acetyltransferase), but genes involved in the synthesis of branched amino acids (e.g., ketol-acid reductoisomerase and acetohydroxyacid synthase) were downregulated. Of the 66 downregulated genes, transcripts of 36 were reduced below the detection limit of 20

Table 3. Affymetrix GeneChip for Maize (Subset)

Row	Accession No.	BLAST Name[a]	Functional Classification	W64A	*su1*	*o1*	*o2*	*o5*	*o9*	*o11*	*Mc*	*fl2*
1	BM500743	trpA gene	Amino acid metabolism	20	20	20	181	58	20	20	20	20
2	BM500953	Tyr/dopa decarboxylase	Amino acid metabolism	20	20	20	94	58	441	25	70	20
3	BM500987	Ser acetyltransferase	Amino acid metabolism	20	20	20	111	20	20	20	20	20
4	BM501487	*S*-Adenosylmethionine decarboxylase	Amino acid metabolism	46	89	197	100	402	537	425	367	264
5	BM500543	Sarcosine oxidase	Amino acid metabolism	51	25	30	90	120	83	392	96	29
6	BM501337	Asp aminotransferase	Amino acid metabolism	63	94	511	52	244	269	462	425	590
7	BM500167	*S*-Adenosyl-L-homocysteine hydrolase	Amino acid metabolism	71	70	307	20	792	954	804	638	308
8	BM500817	*S*-Adenosylmethionine decarboxylase	Amino acid metabolism	102	171	519	121	814	1146	1402	843	619
9	BM501219	Tryp synthase	Amino acid metabolism	138	134	85	20	51	91	106	56	113
10	BM501134	γ Glutamylcysteine synthetase	Amino acid metabolism	139	121	174	42	120	173	269	160	186
11	BM500847	Acetohydroxyacid synthase	Amino acid metabolism	188	188	131	20	131	151	178	104	78
12	BM500837	Ketol-acid reductoisomerase	Amino acid metabolism	206	148	136	34	172	172	222	142	95
13	BM500711	Ala aminotransferase	Amino acid metabolism	282	302	66	20	78	30	283	202	384
14	BM500771	Glyceraldehyde-3-phosphate dehydrogenase	Carbohydrate metabolism	20	94	185	20	190	131	325	138	161
15	BM501023	Hexokinase 1	Carbohydrate metabolism	40	27	122	45	39	21	40	158	183
16	BM500883	Alcohol dehydrogenase	Carbohydrate metabolism	64	54	125	20	123	145	410	58	106
17	BM501055	Aldehyde dehydrogenase	Carbohydrate metabolism	64	64	32	249	137	199	98	107	99
18	BM500651	Oxoglutarate dehydrogenase-like	Carbohydrate metabolism	72	82	185	47	137	227	213	158	254
19	BM500848	Starch synthase isoform	Carbohydrate metabolism	96	81	65	20	72	41	49	26	70
20	BM500415	UDP-Glc dehydrogenase	Carbohydrate metabolism	104	93	126	20	351	481	296	152	20
21	BM500412	Suc synthase 2 (Sus1) gene	Carbohydrate metabolism	108	125	142	20	317	376	332	239	59
22	BM500318	Cinnamyl alcohol dehydrogenase	Carbohydrate metabolism	110	107	219	150	468	600	484	388	100
23	BM500904	Phosphoglucomutase 1	Carbohydrate metabolism	121	204	430	230	949	951	896	826	226
24	BM500521	Starch synthase I precursor (Ss1)	Carbohydrate metabolism	166	162	197	20	138	191	123	142	122
25	BM500559	ADP-Glc pyrophosphorylase small subunit	Carbohydrate metabolism	187	167	57	20	94	109	145	86	62
26	BM500514	Su1p (Sugary1)	Carbohydrate metabolism	202	180	438	398	498	575	472	311	331
27	BM500437	Aldehyde dehydrogenase homolog	Carbohydrate metabolism	237	197	192	30	243	318	480	279	177
28	BM500339	Alcohol dehydrogenase	Carbohydrate metabolism	363	363	324	400	486	572	958	300	160
29	BM500906	Starch-branching enzyme II	Carbohydrate metabolism	372	309	532	1155	566	583	682	464	349
30	BM500488	ADP-Glc pyrophosphorylase	Carbohydrate metabolism	554	523	721	86	677	707	652	679	532
31	BM500477	brittle-1 protein (bt1)	Carbohydrate metabolism	1105	1073	1096	1508	1389	1558	2016	1381	920
32	BM500800	Aldolase	Carbohydrate metabolism	1212	1208	642	683	1425	1554	1463	1381	1122
33	BM500523	Orthophosphate dikinase	Carbohydrate metabolism	1267	1123	484	20	648	1017	1343	781	892
34	BM501186	Enolase	Carbohydrate metabolism	1297	1363	390	516	1275	1363	1865	1584	770
35	BM501158	Cinnamyl alcohol dehydrogenase	Cell wall synthesis/turnover	20	21	57	79	78	129	99	65	27
36	BM501225	Xyloglucan endotransglycosylase	Cell wall synthesis/turnover	20	20	20	162	22	20	20	36	31
37	BM500217	Gly-rich RNA binding protein	Cell wall synthesis/turnover	27	191	97	103	265	518	284	283	48
38	BM500272	β-Glucosidase	Cell wall synthesis/turnover	28	29	108	20	90	151	156	68	62
39	BM501129	GDP-D-mannose-4,6-dehydratase	Cell wall synthesis/turnover	30	29	124	20	20	20	42	42	20
40	AW057082	D-Arabino-heptulosonate phosphate synthase	Cell wall synthesis/turnover	32	20	239	51	212	374	414	190	187
41	BM500683	UDP-Glc dehydrogenase	Cell wall synthesis/turnover	69	117	20	20	235	285	161	42	20
42	BM500275	Hyp-rich glycoprotein	Cell wall synthesis/turnover	179	165	3154	46	3571	4925	4973	3593	429
43	BM501036	*O*-Methyltransferase (OMT)	Cell wall synthesis/turnover	200	246	357	20	314	789	425	187	20
44	BM500432	UDP-Glc dehydrogenase	Cell wall synthesis/turnover	214	187	614	514	1433	1548	1241	939	313
45	BM501403	Hyp-rich glycoprotein	Cell wall synthesis/turnover	239	873	1639	43	2069	2543	3814	2107	904
46	BM500950	β-glucosidase	Cell wall synthesis/turnover	353	369	409	1209	602	539	518	2297	1664
47	BM500473	Gly-rich protein	Cell wall synthesis/turnover	1178	1216	1974	2172	2623	3279	3513	2590	3038
48	BM501103	β-6 tubulin	Cytoskeleton	154	163	100	20	142	187	158	149	53
49	BM500264	Actin (Maz87)	Cytoskeleton	183	242	495	161	623	608	768	481	634
50	BM501270	MAIZE ACTIN 1	Cytoskeleton	200	209	108	20	141	144	196	151	180
51	BM500769	α-Tubulin 3	Cytoskeleton	360	1180	980	129	1292	1824	1420	950	1055
52	BM500192	lojap protein	Energy/respiration	20	20	20	462	242	185	205	167	20
53	BM500845	ATPase	Energy/respiration	28	26	82	20	123	138	237	133	62
54	BM500977	ELECTRON TRANSFER FLAVOPROTEIN	Energy/respiration	120	117	159	139	91	20	356	275	116
55	BM500258	Ubiquinol–cytochrome *c* reductase	Energy/respiration	679	679	442	1767	903	910	963	1004	432
56	BM500731	*Zea mays* ribsomal protein S4	Transcription/translation	20	53	36	20	63	94	95	258	37
57	BM501050	Atp-dependent RNA helicase	Transcription/translation	20	20	68	20	128	145	223	109	49
58	BM501092	OsGRP2	Transcription/translation	29	508	147	20	742	900	867	372	144
59	BM500576	MCM2-related protein	Transcription/translation	32	28	20	134	47	77	151	66	55
60	BM501003	Ribosomal protein L19	Transcription/translation	39	30	47	154	114	108	145	107	56
61	BM501413	SnoRNP protein	Transcription/translation	40	41	28	36	162	151	294	97	20
62	BM500137	Box protein	Transcription/translation	49	55	103	178	203	265	122	137	43

Continued

Table 3. (continued).

Row	Accession No.	BLAST Name[a]	Functional Classification	W64A	*su1*	*o1*	*o2*	*o5*	*o9*	*o11*	*Mc*	*fl2*
63	BM500418	WZF1	Transcription/translation	53	47	100	188	187	135	158	193	83
64	BM500213	CREB binding protein	Transcription/translation	99	88	135	140	40	364	293	320	207
65	BM500199	Ribosome-associated protein p40	Transcription/translation	102	165	233	97	522	631	642	435	193
66	BM500669	Ribosomal protein S25	Transcription/translation	102	99	52	300	141	116	250	135	61
67	BM500923	SRp55-2	Transcription/translation	111	118	87	20	141	90	308	97	146
68	BM501412	H2B histone	Transcription/translation	123	102	49	394	686	466	812	146	39
69	BM500256	Homeobox protein	Transcription/translation	133	129	174	20	85	199	224	239	213
70	BM500821	14-3-3 protein	Transcription/translation	152	134	133	20	137	217	217	172	156
71	BM500293	Box protein	Transcription/translation	156	169	67	20	222	339	169	99	20
72	BM500722	Ribosomal protein L13a	Transcription/translation	159	182	187	205	536	643	650	492	176
73	BM500259	Translation initiation factor 6	Transcription/translation	168	178	223	20	351	406	473	352	217
74	BM500831	Elongation factor 1-α (EF1-A)	Transcription/translation	171	236	657	20	1385	1454	2069	1196	469
75	BM500246	Similar to apoptosis protein MA-3 gb	Transcription/translation	192	200	404	52	256	319	386	771	550
76	BM500839	MNB1b DNA-binding protein	Transcription/translation	201	222	281	302	690	822	704	512	173
77	BM500995	Unknown, group 1935337	Transcription/translation	202	191	195	138	227	380	444	386	73
78	BM500277	Ribosomal protein	Transcription/translation	203	214	90	20	157	20	424	36	57
79	BM501108	Elongation factor 1 β	Transcription/translation	228	286	288	20	536	376	797	280	299
80	BM500726	PVPR3	Transcription/translation	241	258	154	20	174	205	210	133	199
81	CAA34614	Maize Opaque (O2)	Transcription/translation	337	312	770	69	272	367	589	445	442
82	BM500191	Histone H1	Transcription/translation	364	383	312	816	480	152	503	259	176
83	BM500144	Acidic ribosomal protein P1a	Transcription/translation	452	405	578	644	1355	1300	1953	1117	208
84	BM500775	60S RIBOSOMAL PROTEIN L10	Transcription/translation	594	620	685	889	1255	1493	2078	1189	1155
85	BM500450	Elongation factor 1 β	Transcription/translation	640	684	1017	199	891	1129	1653	861	1257
86	BM500766	H2B histone	Transcription/translation	642	710	614	885	1352	1461	1331	930	632
87	BM501385	40S ribosomal protein S5	Transcription/translation	1057	1051	529	1398	1574	1607	1908	1071	543
88	BM500878	Ribosomal protein L10a	Transcription/translation	1134	1135	914	620	683	1051	1461	807	659
89	BM500846	TCTP (apoptosis inhibitor)	Transcription/translation	1170	1140	587	1387	974	894	1148	1003	1216
90	BM500802	Cyc07	Transcription/translation	1453	1516	1316	947	1776	2335	3004	1830	929
91	BM500355	In2-1 mRNA	Herbicide response	20	20	20	132	22	33	64	61	50
92	BM501139	Tonoplast aquaporin	Membrane transport	20	20	20	138	20	50	20	24	20
93	BM501189	PTR (*Hordeum vulgare*)	Membrane transport	20	20	29	125	20	20	20	29	20
94	BM073335	Suc transporter	Membrane transport	23	24	77	30	99	143	104	102	70
95	BM501492	Mitochondrial phosphate transporter	Membrane transport	141	162	190	294	573	626	579	520	95
96	BM500755	Adenine nucleotide translocator	Membrane transport	311	319	461	303	950	1035	1069	749	395
97	BM501130	Aquaporin	Membrane transport	371	356	249	769	344	311	294	406	42
98	BM501391	Aquaporin	Membrane transport	2241	2055	2201	5091	2165	2673	3271	2078	916
99	BM500801	Fer1 gene	Metabolism/oxidoreductase	34	34	39	145	42	80	56	61	23
100	BM500215	Cytochrome b_5 reductase	Metabolism/oxidoreductase	74	72	150	263	221	252	226	197	126
101	BM500371	Cytochrome P450	Metabolism/oxidoreductase	97	72	95	373	155	142	179	135	138
102	BM500860	Cytosolic ascorbate peroxidase	Metabolism/oxidoreductase	160	211	315	195	434	533	405	423	302
103	BM500873	Glutathione peroxidase	Metabolism/oxidoreductase	255	262	204	337	274	380	330	288	125
104	BM501155	Glutathione *S*-transferase III	Metabolism/oxidoreductase	617	617	433	2029	905	967	720	750	174
105	BM500211	hsp70	Molecular chaperonin	20	222	144	52	142	134	94	146	304
106	BM501102	Calreticulin	Molecular chaperonin	20	120	87	20	110	133	195	264	79
107	BM501110	Heat-shock protein 60	Molecular chaperonin	20	20	20	20	20	20	31	403	225
108	BM500968	T complex polypeptide 1	Molecular chaperonin	31	28	76	294	214	261	476	159	29
109	BM500857	Hsp82	Molecular chaperonin	37	141	155	21	161	175	298	105	78
110	BM500768	hsp70	Molecular chaperonin	48	568	377	20	524	676	824	570	189
111	BM500396	BiP	Molecular chaperonin	49	105	76	156	133	199	170	729	676
112	BM500525	HSP90	Molecular chaperonin	55	158	216	210	294	276	475	845	348
113	BM500334	BiP	Molecular chaperonin	66	51	91	98	66	52	20	756	984
114	BM500779	PDI	Molecular chaperonin	74	131	618	20	836	1040	1141	1628	1930
115	BM501499	Low molecular mass HSP	Molecular chaperonin	165	174	170	427	432	443	296	710	244
116	BM500815	Cyclophilin	Molecular chaperonin	406	713	888	514	2070	3013	2569	1791	1640
117	BM500928	Immunophilin	Molecular chaperonin	553	610	679	536	905	1142	1196	779	573
118	BM500673	Stearoyl–acyl carrier protein desaturase	Oil metabolism	93	92	60	20	52	69	108	35	20
119	BM500156	Lipase	Oil metabolism	213	227	188	26	310	492	457	134	103
120	BM501215	Cys endopeptidase EP-A	Protein turnover	20	20	25	186	144	50	40	115	20
121	BM500457	PROTEASOME COMPONENT C2	Protein turnover	31	20	20	239	152	148	134	174	116
122	BM500666	COP9	Protein turnover	43	41	76	233	122	114	177	151	72
123	BM500734	MPI	Protein turnover	67	74	140	312	169	208	175	158	136
124	BM500900	26S protease subunit	Protein turnover	68	96	128	278	172	170	211	247	142
125	BM500238	MubG9 ubiquitin	Protein turnover	122	138	332	20	191	339	375	367	503

Continued

Table 3. (continued).

Row	Accession No.	BLAST Name[a]	Functional Classification	W64A	*su1*	*o1*	*o2*	*o5*	*o9*	*o11*	*Mc*	*fl2*
126	BM501479	Protease inhibitor	Protein turnover	124	277	265	20	875	1078	517	153	264
127	BM501085	Subtilisin	Protein turnover	489	553	828	541	457	563	525	3832	5822
128	BM500282	Ubiquitin–conjugating enzyme	Protein turnover	1006	1026	663	821	542	614	697	645	1570
129	BM500454	Polyubiquitin	Protein turnover	1110	1229	1695	654	1083	1656	1593	1765	2666
130	BM500849	Proteinase inhibitor	Protein turnover	1590	1494	5846	1023	3671	4580	3613	3472	1190
131	BM500738	Subtilisin-chymotrypsin inhibitor	Protein turnover	2024	2012	2257	3928	557	1502	3747	4353	4419
132	AF371280	Hageman factor inhibitor	Protein turnover	4881	4908	6908	2610	5084	7393	7689	3661	3067
133	BM500917	UDP-glycose:flavonoid glycosyltransferase	Secondary metabolism	55	41	587	90	480	501	560	755	95
134	BM500335	UTP-Glu glucosyltransferase	Secondary metabolism	103	105	81	433	248	239	195	229	192
135	BM501149	Ferripyochelin binding protein	Secondary metabolism	118	92	96	359	157	176	152	147	318
136	BM500649	4-Coumarate:CoA ligase	Secondary metabolism	122	122	172	499	355	275	337	443	20
137	BM500713	Dihydroflavonol 4-reductase	Secondary metabolism	142	114	136	68	64	71	118	101	127
138	BM500528	Isopentenyl diphosphate isomerase I	Secondary metabolism	195	249	326	38	254	380	378	239	634
139	BM500165	CHI gene	Secondary metabolism	243	264	286	806	600	726	314	533	76
140	BM500818	Chorismate synthase 1	Secondary metabolism	346	330	259	242	367	452	483	347	139
141	BE997384	Germin-like protein	Seed protein	20	20	47	141	103	163	30	104	20
142	AAA33467	Globulin S (7S-like)	Seed protein	76	65	68	509	80	151	401	377	395
143	AF371265	18-kD δ-zein	Seed protein	163	113	189	20	306	216	757	107	329
144	AF371279	Maize legumin1	Seed protein	1576	1640	2862	1346	2513	3803	4068	1666	1496
145	AF371278	Maize α-globulin	Seed protein	3541	3325	2908	5716	2200	3051	3049	3655	2596
146	AF371263	50-kD γ-zein	Seed protein	4092	3705	4117	3697	927	1520	3074	4250	4399
147	AF371267	19-kD D1 α-zein	Seed protein	4122	3848	3184	3139	1712	2130	3435	4611	4178
148	AF371268	19-kD D2 α-zein	Seed protein	4309	4130	3717	1595	818	1509	2598	4264	4458
149	AF371274	22-kD α-zein Z1	Seed protein	4823	4386	6651	20	2650	4218	5935	6625	4996
150	AF371277	22-kD α-zein Z5	Seed protein	5756	5489	4761	20	20	139	4165	4918	3325
151	AF371266	10-kD δ-zein	Seed protein	6168	6056	6618	1285	7407	8043	7483	7396	6896
152	AF371264	15-kD β-zein	Seed protein	7752	7995	6608	1562	5247	6051	6543	4925	5355
153	AF371269	19-kD B1 α-zein	Seed protein	8577	8605	7049	8533	5681	7994	8191	9437	5578
154	AF371271	19-kD B3 α-zein	Seed protein	8809	9086	9031	7157	7552	10548	9302	8676	6286
155	AF371270	19-kD B2 α-zein	Seed protein	9279	9299	7950	7888	6212	8971	7696	8921	5074
156	AF371276	22-kD α-zein Z4	Seed protein	9843	9782	7297	3596	5807	8922	7977	10423	7806
157	AF371275	22-kD α-zein Z3	Seed protein	9994	10001	7735	1628	5497	7923	7454	9784	6962
158	AF371261	27-kD γ-zein	Seed protein	11228	11362	10745	9442	9757	11996	12695	11041	6716
159	AF371262	16-kD γ-zein	Seed protein	13984	14157	12420	16463	9774	12844	11086	12880	7793
160	BM500803	Ras GTPase-activating protein	Signal transduction	20	20	20	20	20	20	20	198	20
161	BM500881	ATPase	Signal transduction	20	20	91	39	86	104	114	97	74
162	BM501345	Phospholipase D	Signal transduction	20	20	41	87	62	58	58	360	259
163	BM500957	Ser/Thr protein kinase	Signal transduction	21	24	104	37	58	95	123	216	47
164	BM501160	Mitogen-activated protein kinase kinase 5	Signal transduction	23	20	54	193	143	113	178	61	33
165	BM500243	Ring zinc finger protein	Signal transduction	24	30	55	144	69	64	90	69	53
166	BM500498	Phospholipase D	Signal transduction	31	31	46	150	91	119	82	75	69
167	BM500204	Protein kinase	Signal transduction	46	43	76	184	96	148	104	104	74
168	BM501205	CDPK-related protein kinase	Signal transduction	55	56	26	213	55	40	33	71	66
169	BM500209	ras-like gene	Signal transduction	59	83	91	40	43	65	122	190	200
170	BM501022	Ran protein	Signal transduction	59	62	87	193	152	128	241	169	50
171	BM501053	Kinase associated protein phosphatase (KAPP)	Signal transduction	67	78	203	85	319	466	334	259	86
172	BM501390	Similar to "tub" protein	Signal transduction	75	72	157	166	156	197	195	187	204
173	BM500146	Phytochrome A	Signal transduction	79	64	96	301	159	203	140	147	100
174	BM500466	Auxin-responsive GH3 protein	Signal transduction	83	122	309	131	339	484	472	176	272
175	BM500841	14-3-3 protein	Signal transduction	94	138	439	20	382	630	518	618	446
176	BM501156	Phosphatase like	Signal transduction	114	103	207	377	258	229	203	277	66
177	BM500705	GUANINE NUCLEOTIDE BINDING protein	Signal transduction	125	128	253	281	464	502	611	399	232
178	BM501305	GDP dissociation inhibitor protein	Signal transduction	142	121	79	20	130	97	179	99	61
179	BM500384	Receptor kinase	Signal transduction	144	176	303	206	412	533	477	394	272
180	BM501263	Apospory-associated protein	Signal transduction	164	169	106	58	97	120	195	162	196
181	BM501224	ADP-ribosylation factor 1	Signal transduction	204	245	396	470	515	709	567	654	768
182	BM500556	MEGF6	Signal transduction	241	252	128	24	650	1270	633	660	40
183	BM501371	Apospory-associated protein	Signal transduction	249	274	306	26	359	361	386	458	413
184	BM500976	Protein kinase ARSK1	Signal transduction	303	240	108	20	175	314	452	184	153
185	BM500328	ras-related protein	Signal transduction	335	673	452	416	916	933	809	755	786
186	BM500798	Protein kinase C Inhibitor	Signal transduction	336	330	156	362	327	385	383	238	121
187	BM501363	14-3-3 protein	Signal transduction	405	450	542	406	1001	1100	1191	1322	889
188	BM501116	3-Hydroxy-3-methylglutaryl-CoA	Sterol metabolism	28	20	20	141	43	48	20	60	20

Continued

Table 3. (continued).

Row	Accession No.	BLAST Name[a]	Functional Classification	W64A	*su1*	*o1*	*o2*	*o5*	*o9*	*o11*	*Mc*	*fl2*
189	BM501086	SAM sterol-C-methyltransferase	Sterol metabolism	57	182	139	279	205	211	279	325	160
190	BM500315	C-24 sterol methyltransferase	Sterol metabolism	229	222	124	28	276	307	354	161	80
191	AAA33517	NADPH HC-toxin reductase	Stress/defense response	20	20	34	134	56	53	57	88	31
192	BM500346	Flavonol 4′-sulfotransferase	Stress/defense response	20	20	20	167	20	20	20	34	25
193	BM500424	Wound–induced protein	Stress/defense response	20	109	20	20	20	242	2568	541	79
194	BM501089	Anthranilate/benzoyltransferase	Stress/defense response	20	20	68	111	100	109	75	20	60
195	BM501467	Phe ammonia-lyase	Stress/defense response	20	28	76	20	98	231	157	99	20
196	BM500682	119.5-kD protein (uvrA region)	Stress/defense response	22	47	24	120	117	51	63	20	20
197	BM501411	32.6-kD jasmonate-induced protein	Stress/defense response	36	49	96	20	218	304	356	148	28
198	BM500898	Flavonol synthase	Stress/defense response	51	51	79	208	155	136	117	148	44
199	BM500720	Peroxidase ATP22a	Stress/defense response	61	62	108	275	74	117	86	128	84
200	BM500210	Heat-shock transcription factor21	Stress/defense response	72	67	128	357	181	177	168	181	80
201	BM501480	Stress-related protein	Stress/defense response	72	195	106	28	708	855	477	193	33
202	BM500721	Allene oxide synthase	Stress/defense response	73	67	118	358	237	227	288	280	133
203	BM501266	Osmotin-like protein	Stress/defense response	78	102	171	71	299	355	390	109	77
204	BM500875	Hs1pro-1related protein	Stress/defense response	90	92	47	261	121	123	112	144	145
205	BM500706	AIG2-like protein	Stress/defense response	93	94	80	120	49	104	38	56	59
206	BM500142	Fis1 gene product	Stress/defense response	103	114	70	20	91	158	101	79	41
207	BM501245	Peroxidase ATP20a	Stress/defense response	129	111	611	575	484	1167	1217	719	169
208	BM500545	Antifungal zeamatin-like	Stress/defense response	168	163	152	1091	128	297	301	313	396
209	BM500627	Prohibitin	Stress/defense response	169	140	87	404	502	421	687	513	103
210	BM501164	Peroxidase ATP6a	Stress/defense response	195	173	244	645	333	521	391	366	231
211	BM500401	Cell death protein	Stress/defense response	202	157	247	653	387	423	501	474	355
212	BM501039	BET1	Stress/defense response	229	534	263	282	1063	1132	514	279	444
213	BM500239	Chitinase B	Stress/defense response	284	277	179	272	136	84	206	150	227
214	BM501025	Duplicated domain structure protein	Stress/defense response	297	428	279	155	291	168	493	1373	717
215	BM500550	Class II metallothionein	Stress/defense response	357	366	101	139	91	104	144	151	394
216	BM500955	Phe ammonia lyase	Stress/defense response	371	332	1043	623	1406	2159	1885	1218	443
217	BM501062	γ-Zeathionin 1	Stress/defense response	523	517	173	670	20	20	91	83	700
218	BM501377	Ascorbate peroxidase	Stress/defense response	630	672	991	559	1174	1506	1551	1231	760
219	BM500522	Stress-related protein	Stress/defense response	635	603	349	797	230	337	321	227	672
220	BM501313	Metallothionein	Stress/defense response	807	825	559	253	460	1062	1524	719	748
221	BM501060	γ-Zeathionin 2	Stress/defense response	1712	1727	836	1814	62	146	682	430	2722
222	AAA33508	RIP	Stress/defense response	1906	1792	700	618	787	1060	1588	2023	1908
223	AW257994	7S Globulin/antimicrobial peptide	Stress/defense response	2307	2222	1283	2945	231	260	613	681	4417
224	BM500728	Unknown	Unknown	27	28	42	205	39	64	43	51	99
225	BM500653	Unknown	Unknown	33	48	128	20	20	20	86	61	20
226	BM501204	Unknown	Unknown	39	62	78	269	133	175	111	143	98
227	BM501181	Unknown	Unknown	40	35	88	75	125	226	147	115	71
228	BM501038	Unknown	Unknown	46	94	341	20	761	1214	310	271	71
229	BM500905	Unknown	Unknown	47	45	52	216	142	144	313	90	27
230	BM501242	Unknown	Unknown	49	49	59	345	269	301	254	297	103
231	BM501506	Tpc70 protein (*Tradescantia paludosa*)	Unknown	50	49	52	212	94	77	84	110	63
232	BM500517	(AC002131) contains similarity to BAP31 protein gb	Unknown	84	84	73	217	99	142	189	266	218
233	BM500736	Unknown contig, group 2043014	Unknown	101	95	57	240	137	41	129	164	116
234	AI065441	(AC004392) EST gb	Unknown	183	119	253	20	294	194	182	386	134
235	BM500909	(AL022198) hypothetical protein	Unknown	198	455	339	248	753	891	737	187	916
236	BM500764	Unknown contig, group 1778124	Unknown	253	252	131	478	150	111	162	175	149

List of genes and gene expression intensities in 18-DAP endosperm of W64A+, W64A *su1*, and W64A opaque mutants.

[a]The designations of BLAST names are based on the unedited names of the corresponding most similar BLAST hits in GenBank.

expression intensity units. The downregulated genes in *o2* accounted for ~30% of the expressed gene intensity units in W64A+.

Figure 4 shows a data set illustrating the effect of the six other opaque mutants on gene expression in 18-DAP endosperm (*DeB30* was not included in this analysis because it was unavailable during this growing season). A cursory examination of the scatterplots demonstrates that these mutants, like *o2*, are much more pleiotropic than *su1*. Of the six opaque mutants, *o5*, *o9*, *o11*, and *fl2* showed the greatest variation in gene expression relative to the wild type, with regression analysis values of approximately $R^2 = 0.85$; *o1* and *Mc* were more similar to the wild type, with regression analysis values of $R^2 = 0.93$. In *o1*, 35 genes

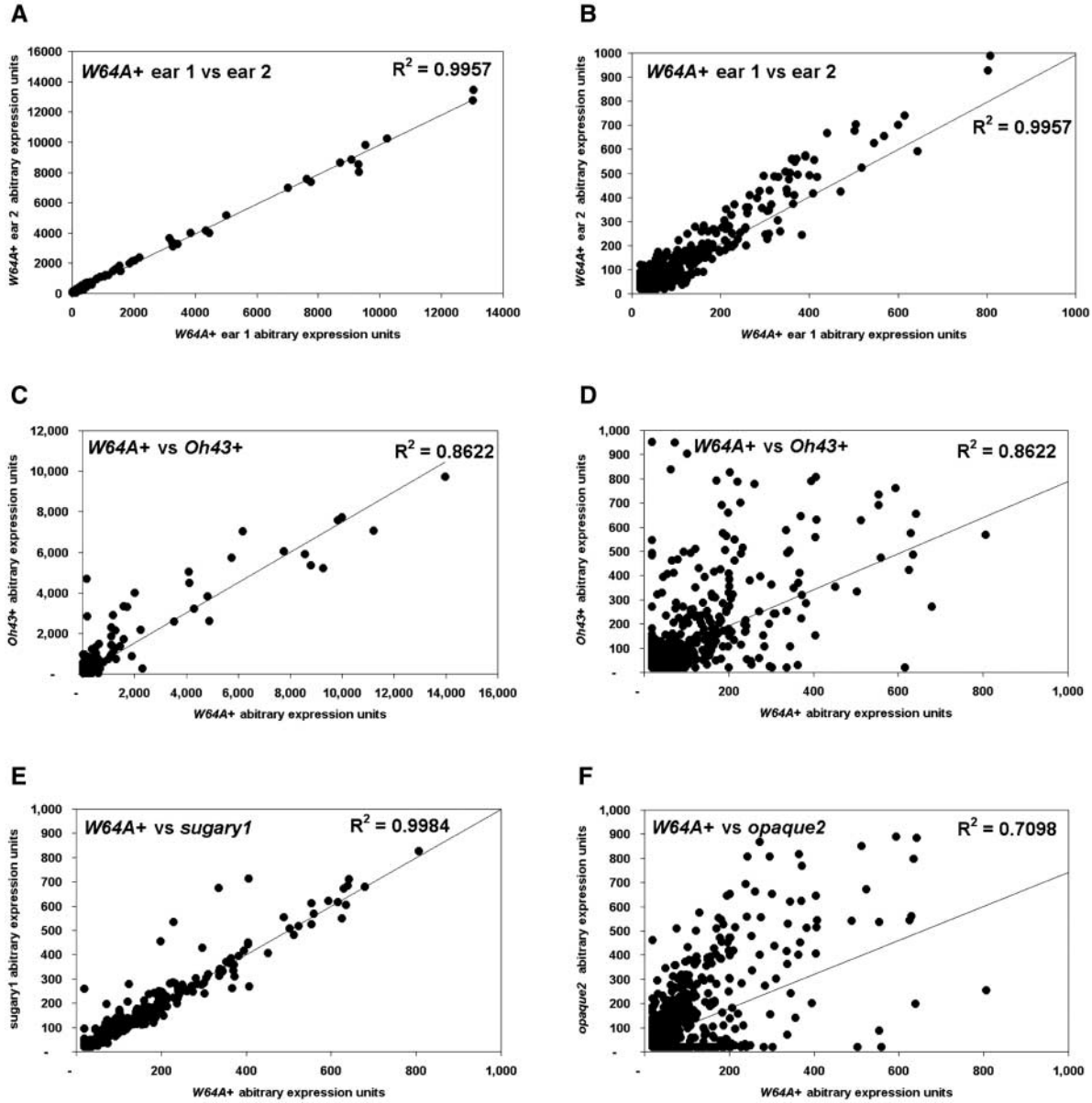

Figure 3. Assessment of Endosperm Gene Expression Using Maize Affymetrix GeneChip Microarrays.

Each graph shows a scatterplot and a linear regression plot comparing expression intensities of endosperm-specific transcripts. R^2 is the coefficient of determination.

(A) Comparison of endosperm-specific transcripts obtained from two independent ears of W64A+.

(B) Expanded view of the plot shown in **(A)**, with expression intensities between 20 and 1000 arbitrary units to emphasize expression intensity differences between the two ears.

(C) Comparison of endosperm-specific transcripts obtained from the inbred lines W64A+ and Oh43+.

(D) Expanded view of the plot shown in **(C)**, with a maximum of 1000 arbitrary units.

(E) Comparison of endosperm-specific transcripts obtained from W64A+ and from the starch biosynthetic mutant W64A *su1*. The plot is an expanded view with a maximum of 1000 arbitrary units.

(F) Comparison of endosperm-specific transcripts obtained from W64A+ and the W64A *o2* mutant. The plot is an expanded view with a maximum of 1000 arbitrary units.

were upregulated more than threefold (see supplemental data online), and most of these encode putative chaperones (HSP90, HSP82, HSP70 [two different accessions], calreticulin, and petide disulfide isomerase) and stress-related proteins (peroxidase, proteinase inhibitor, and Gly- and Hyp-rich proteins [three different accessions]). Transcripts of the latter three genes were increased dramatically in *o1* relative to the wild type. The expression of one gene encoding eEF1A was increased fourfold, and expression of a gene encoding Asp aminotransferase was increased eightfold. Twenty-two genes, including Ala aminotransferase, two ribosomal proteins, zeathionin genes (two different accessions), orthophosphate dikinase, and RIP, were downregulated at least twofold in *o1*. There were no large changes in seed storage protein gene expression in *o1*.

In *o5*, the expression of 67 genes was increased more than threefold relative to the wild type. *o5* showed upregulated expression of many molecular chaperones and the stress-related genes upregulated in *o1*, but in addition to these, expression of HSP22, TCP1, *cis-trans* prolyl-isomerase (cyclophilin), BET1, and phenylalanine ammonia lyase (PAL) also were increased (see supplemental data online). Other genes upregulated in *o5* include a 14-3-3 homolog, Asp aminotransferase, cytoskeleton-related proteins (α-tubulin, actin, and eEF1A), and legumin1. Among the 26 genes downregulated more than twofold in *o5* are Trp synthase, Ala aminotransferase, metallothionein, ubiquitin-conjugating enzyme, orthophosphate dikinase, RIP, and zeathionin (two different accessions). Several genes encoding zein storage proteins are among those downregulated in *o5*: the 50-kD γ-zein, 19-kD D1 and D2 α-zeins, and four 22-kD α-zeins (*fl2* transcript disappeared, and three others were reduced by half).

In *o9*, the expression of 58 genes was increased more than threefold relative to the wild type (see supplemental data online). Most of these (51) are identical to those upregulated in *o5* (Table 3). Nineteen genes were downregulated more than twofold compared with the wild type, and 17 of these were identical to those affected similarly in *o5*. These included several zein protein genes, the 50-kD γ-zein, and the 19-kD D1 and D2 α-zeins but only one of the 22-kD α-zeins (*fl2*).

Alterations in the expression pattern of genes in *o11* were similar to those in *o5* (62) and *o9* (51), the most upregulated and downregulated genes (77 and 5, respectively) (Table 3; see also supplemental data online). The only downregulated storage protein gene in *o11* encodes the 19-kD D1 α-zein. The legumin1 gene and the 18-kD δ-zein were upregulated.

In *fl2*, the expression of 37 genes was increased threefold relative to the wild type, whereas the expression of 22 genes was reduced at least twofold (see supplemental data online). Among the overexpressed genes are several that encode stress-related transcripts, including PAL, the chaperones affected in *o5*, *o9*, and *o11*, as well as HSP60, a second binding protein accession, and calreticulin. Notably, as a group, the expression of ER-related chaperones was remarkably higher than that in the other opaque mutants (Table 3). Genes encoding cytoskeletal proteins (actin, eEF1A, and α-tubulin) and genes related to protein turnover (polyubiquitin, MUBG9 ubiquitin, and subtilisin-like protease) also were upregulated. Downregulated genes included starch-branching enzyme1, ribosomal proteins, and glutathione *S*-transferase. Water channel protein genes also were downregulated, in contrast to *o2*, in which they were upregulated. The expression of three zein genes was reduced by ~50%: 19-kD Bα-zein, a 22-kD α-zein that is not the *fl2* gene, and the 16-kD γ-zein gene.

Relative to the wild type, there were 57 upregulated genes but only 7 downregulated genes in the *Mc* mutant (see supplemental data online). Genes showing greater than normal levels of expression included stress-related sequences and the chaperones affected in the other opaque mutants, and in particular the putatively ER-localized chaperones affected in *fl2*. Two 14-3-3 gene homologs, as well as a duplicated domain structure protein gene, were expressed at increased levels. Also increased in expression were genes associated with protein turnover, including a 26S protease subunit, subtilisin protease, and polyubiquitin, and genes encoding cytoskeletal proteins, such as eEF1A. Conspicuously, there were no zein genes among the five sequences downregulated in *Mc*.

A cluster analysis (Eisen et al., 1998) of the gene expression phenotypes of these mutants revealed a close relationship between *o5*, *o9*, and *o11*; the *fl2* and *Mc* mutants also were related. The *o1* and *o2* mutants showed no meaningful grouping with the other opaque mutants (data not shown). A pairwise comparison of selected mutants is shown in Figure 5. The comparison of gene expression in *o5* and *o2* ($R^2 = 0.66$) showed that these mutants are as dissimilar to one another as they are to the wild type (Figure 5A). By contrast, comparison of *o5* and *o9* ($R^2 = 0.93$; Figure 5B) and *o5* and *o11* ($R^2 = 0.98$; data not shown) showed that these mutants share fundamentally similar patterns of gene expression. Figure 5C shows a comparison of the gene expression patterns in *o2* and *fl2*. In this case, the coefficient of determination ($R^2 = 0.56$) for the scatterplot shows that these mutants induce quite different patterns of gene expression in 18-DAP endosperm. The opaque mutant with the closest relation to *fl2* is *Mc* (Figure 5D). The coefficient of determination between *fl2* and the wild type is $R^2 = 0.84$, and that between *fl2* and *Mc* is $R^2 = 0.89$. This finding indicates that *fl2* and *Mc* share a subset of genes with expression patterns that are not similar to those of the wild type. This conclusion is corroborated by comparison of the gene expression data in Table 3.

DISCUSSION

The objective of this research is to understand the cause of the starchy kernel phenotype in maize opaque endosperm mutants. In the case of *o2* and *fl2*, the basis of the genetic

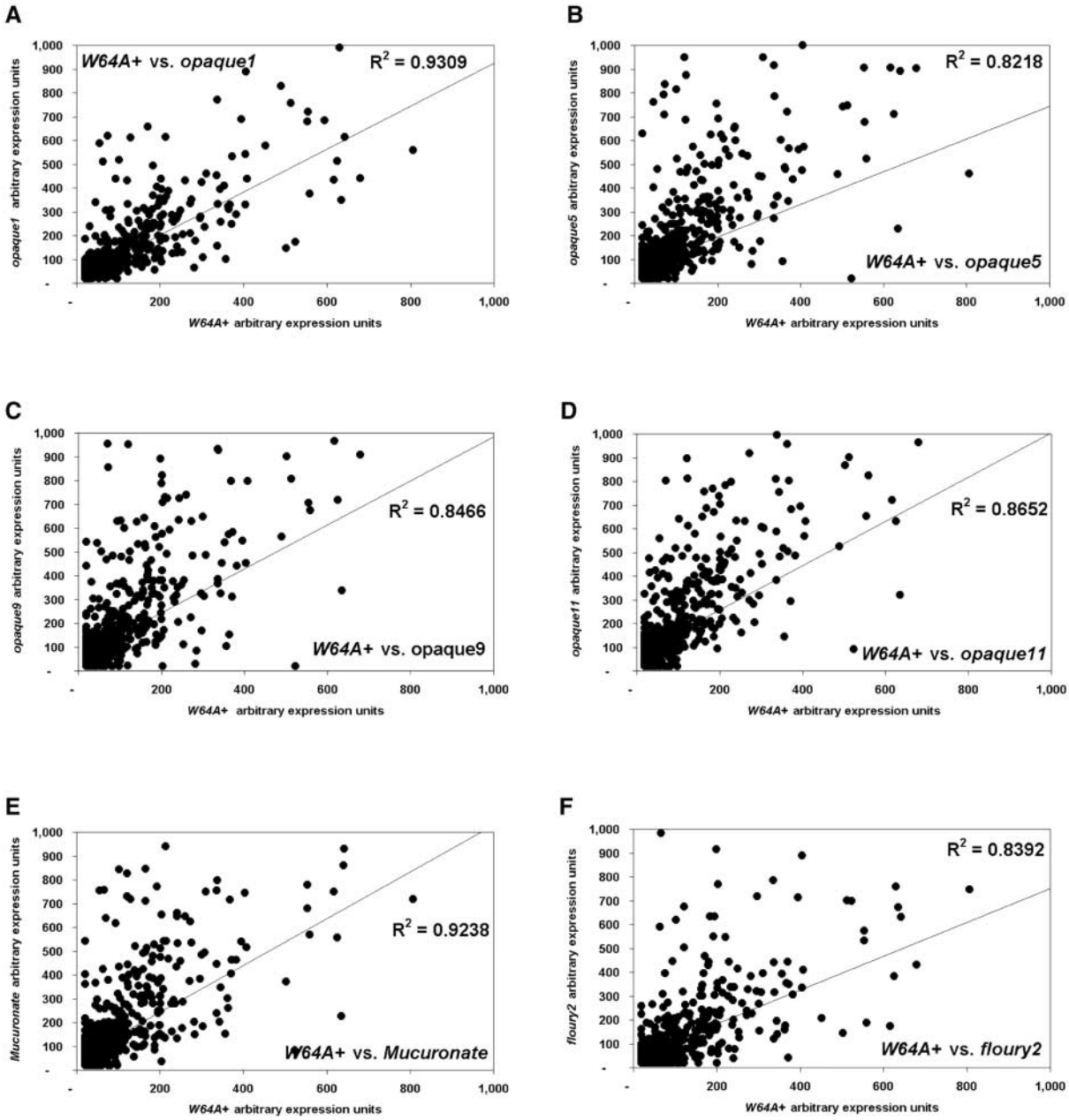

Figure 4. Comparisons of Endosperm Gene Expression between W64A+ and the Nearly Isogenic Opaque Mutants Using Maize Affymetrix GeneChip Microarrays.

Each graph is a scatterplot and a linear regression plot comparing expression intensities of endosperm-specific transcripts. The plots show a maximum of 1000 arbitrary expression units to emphasize expression intensity differences. R^2 is the coefficient of determination.

(A) Comparison between W64A+ and W64A *o1*.

(B) Comparison between W64A+ and W64A *o5*.

(C) Comparison between W64A+ and W64A *o9*.

(D) Comparison between W64A+ and W64A *o11*.

(E) Comparison between W64A+ and W64A *Mc*.

(F) Comparison between W64A+ and W64A *fl2*.

defect is known (Schmidt et al., 1990; Coleman et al., 1997b), but the mechanisms by which these two very different types of mutations result in a similar mature endosperm phenotype is unclear. To compare the patterns of gene expression and protein synthesis in *o2* and *fl2* with those of other opaque mutants, it was essential that the mutations be introgressed uniformly into a common genetic background. The nearly isogenic W64A+ and opaque mutant inbred lines were created by recurrent backcrossing, and they are phenotypically uniform and appear to be genetically homogeneous. Besides displaying similar height, leaf shape, and color, as well as a number of other whole-plant phenotypic characteristics, their seeds are similar in size and protein content. These results are expected, because after six backcross generations the mutant inbred lines should share, on average, ~99% of the recurrent parent genome. Most of these mutants show a strict endosperm phenotype, but in the cases of *o5* and *o9*, it is possible that the mutations are not seed specific. These mutant plants show retarded development; consequently, the opaque endosperm phenotype could result from deleterious effects of the *o5* and *o9* mutations on seed development.

Although an opaque phenotype often is tacitly associated with an increased endosperm Lys concentration, a comparison of these mutations in the W64A genetic background revealed marked differences in the contents of essential amino acids, and Lys in particular. The *o1* mutant has an amino acid composition nearly identical to that of the wild type, a result consistent with that of Nelson et al. (1965). Each of the other opaque mutants has a higher endosperm Lys concentration than the wild type, although the increases are not as great as in *o2*. The *o2* mutant has the highest Lys content, followed by *o11*, *DeB30*, and *fl2*. Except for *o1*, the amount of the nonzein protein fraction in these mutants is increased, as in *o2*, and the amount of the zein protein fraction is decreased. Balconi et al. (1998) reported that *o1* increased the endosperm Lys content of the A69Y inbred line as much as *o2*. They also found the Lys contents of A69Y *o9* and *o11* to be significantly higher that those we observed in W64A. The differences between these two sets of data could be explained by the response of the inbred backgrounds to these mutations and, potentially, allelic variation among the mutants. However, like the samples used by Balconi et al. (1998), our *o1*, *o9*, and *o11* mutants were from the Maize Genetic Cooperation (Urbana, IL), and they are likely to result from the same alleles (Neuffer et al., 1997).

Significant differences in total protein and zein proteins were found in most of the opaque mutants. The largest reductions in zein synthesis occurred in the W64A *o2*, *DeB30*, and *fl2* mutants, which had ~35 to 55% of the wild-type level of storage proteins. Zeins in W64A *o5*, *o9*, *o11*, and *Mc* were within 80 to 90% of the amount found in the wild type. Besides *o2* and *fl2*, significant qualitative changes in zein synthesis also were observed in *o5* and *Mc* (see below). We previously identified several wild-type inbred lines that contain less total protein (7 to 9%) and similar amounts of zein proteins (5.5 mg/100 mg of endosperm) as these opaque mutants. Furthermore, the *o1* mutant contains nearly identical amounts of zein and nonzein proteins as the wild type. Consequently, neither the amount of zein protein synthesis nor the reduction in total protein content adequately explains the opaque endosperm phenotype of these mutants.

In only a few of these mutants did we detect considerable qualitative and quantitative differences in individual seed proteins. In *o2* and *fl2*, we observed the well-documented changes in the amount and/or size of the 22-kD α-zeins. We also found a reduction in the amount of 10-kD δ-zein and of 15-kD β-zein in *o2*, which was not reported previously. Likewise, the reduced level of 16-kD γ-zein in *Mc* was not described previously, nor was the detection of polymorphic forms of this protein. Based on our recent experiments, it appears that the *Mc* mutation likely results from a defective allele encoding a 16-kD γ-zein protein (C.-S. Kim, unpublished data). With the exception of *Mc*, we were unable to identify qualitative changes in seed storage proteins that could explain the starchy endosperm phenotype of the other opaque mutants.

An interesting change in one seed protein is the presence of the 18-kD δ-zein in *o5* endosperm (Figure 1). W64A+ and the nearly isogenic opaque mutants did not accumulate detectable levels of the 18-kD δ-zein polypeptide, and these inbred lines appear to express this gene at a low level. However, the 18-kD δ-zein gene in *o5* is an unlikely candidate for a mutated allele of the *O5* gene: the *o5* mutation is associated with a whole-plant phenotype (see above), and the 18-kD δ-zein is expressed exclusively in the endosperm. There are two possible explanations for the higher expression of the 18-kD δ-zein in *o5*. First, the normally suppressed 18-kD δ-zein gene (Swarup et al., 1995) could be derepressed in *o5*, perhaps as a result of the mutation. Second, a strong δ-zein allele could have been carried along during the backcrossing process. A genetic linkage between *o5* and the 18-kD δ-zein gene would not be expected, because the 18-kD δ-zein maps to chromosome 6L and *o5* maps to chromosome 7L (Coleman et al., 1997a; Woo et al., 2001). However, another polymorphism detected in *o5* is an electrophoretically slower migrating α-globulin peptide (Figure 1). The α-globulin and the 18-kD δ-zein loci are linked closely on the long arm of maize chromosome 6 (Woo et al., 2001). This observation implies that these alleles were transmitted from the *o5* donor parent, despite the six backcross generations.

The development of an Affymetrix GeneChip containing maize genes made it possible for us to analyze the patterns of gene expression in these mutants in a much more global manner than was possible by comparing qualitative and quantitative changes in protein and amino acid composition. The use of high-density oligodeoxyribonucleotide microarrays has emerged as an important tool for the simultaneous examination of large numbers of expressed genes (Knight, 2001). However, a major limitation of this technology is its "closed" nature (i.e., only preselected genes are probed,

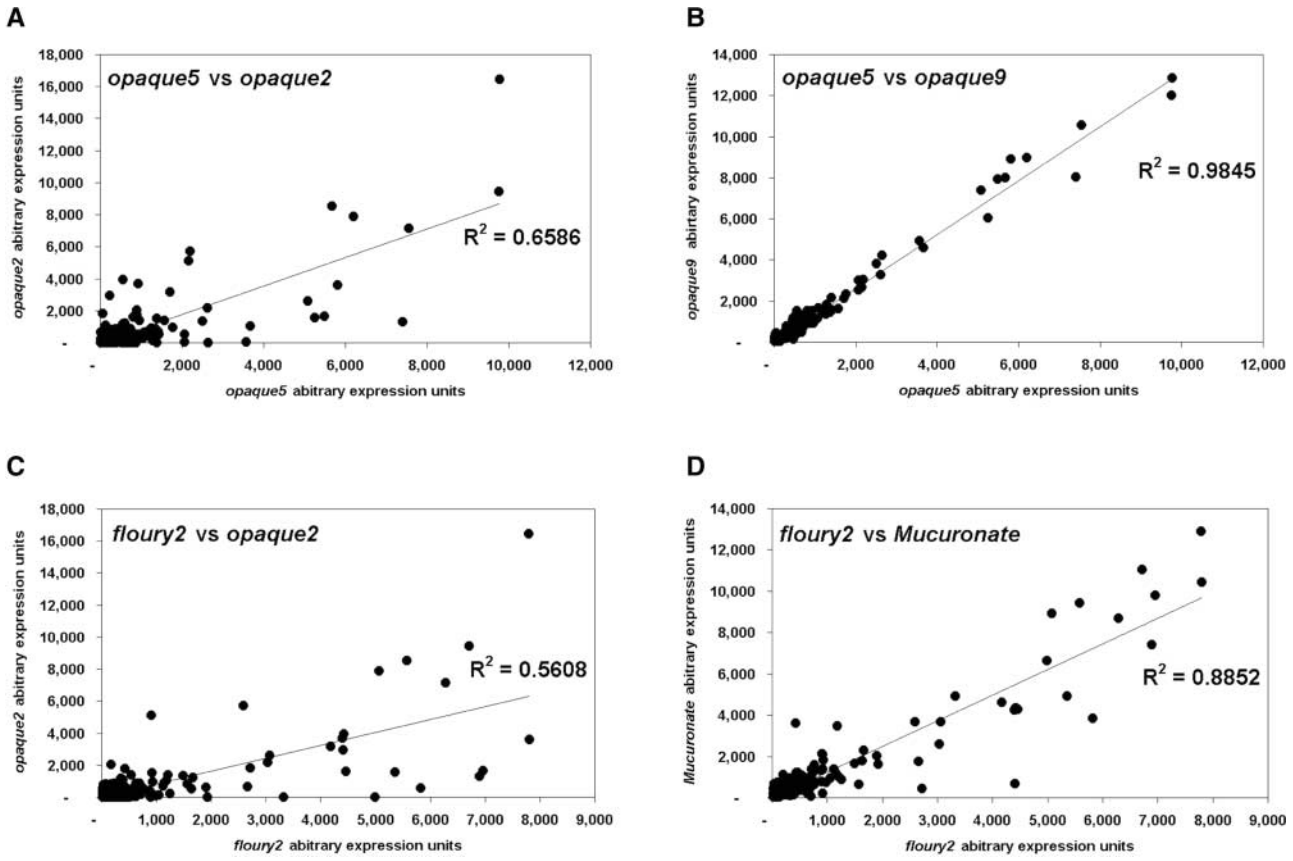

Figure 5. Gene Expression Differences and Similarities between Selected Opaque Mutants.

Each graph is a scatterplot and a linear regression plot comparing expression intensities of endosperm-specific transcripts. R^2 is the coefficient of determination.

(A) Comparison between W64A *o5* and W64A *o2*.

(B) Comparison between W64A *o5* and W64A *o9*.

(C) Comparison between W64A *fl2* and W64A *o2*.

(D) Comparison between W64A *fl2* and W64A *Mu*.

and it is not possible to discover new genes). The maize genome contains an estimated 80,000 expressed genes, and approximately one-fifth of these are transcribed in the endosperm (Woo et al., 2001). Despite a growing collection of maize ESTs in GenBank, only a fraction of the corresponding genes have been sequenced completely. Consequently, it is currently not feasible, technically or economically, to produce microarrays that include the majority of maize genes.

The profile of endosperm transcripts was obtained with an Affymetrix GeneChip microarray based on the sequence information of >1400 maize genes; generally, these are alleles of the B73 inbred line (see Methods). More than 80% of these genes have annotations (i.e., have been characterized functionally in maize or other species and closely match functionally known genes). These genes were selected to cover a wide range of metabolic pathways and cellular and physiological processes (see supplemental data online). The GeneChip also contains probes for members of multigene families, notably, members of the different seed protein gene families (Table 3). The hybridization results show a high degree of resolution between these probes. This specificity illustrates an important advantage of oligodeoxyribonucleotide-derived microarrays compared with arrays that use larger DNA fragments immobilized on glass slides (Knight, 2001). The latter usually do not distinguish between closely related members of multigene families. A disadvantage of the selectivity of GeneChips, at least for the types of experiments conducted here, is the allele sensitivity of the probes. Our experiments were performed with W64A

cRNA samples, but the majority of the probes on the microarray were derived from B73 alleles. When scanned after hybridization, ~20% of these probes produced negative values (Table 2). This occurred because of the stronger hybridization signals obtained with the control probes for each gene (i.e., from the sets of mismatched oligodeoxyribonucleotides). Consequently, the W64A samples contained a number of cRNA species (alleles or homologs) that matched more closely the control than the target probes. Because of this ambiguity, we did not consider such results informative for this analysis. This suggests a general difficulty with array studies that rely on exact sequences and knowledge of homologs.

ESTs corresponding to the majority of genes (or their alleles) on the maize GeneChip are represented in maize endosperm cDNA libraries, and the level of transcripts corresponding to several of these genes was studied previously in detail (Woo et al., 2001). Therefore, the use of the maize GeneChip to examine endosperm gene expression appeared to be feasible, and the presence of well-characterized genes provided important experimental controls.

The analysis of the GeneChip hybridization results demonstrated that these experiments provide a reasonably thorough assessment of endosperm mRNA transcript abundance. The cRNA was synthesized with biotin-labeled CTP and UTP nucleotides; consequently, the labeling differences between cRNA species of varying GC content were minimal. The majority of the oligonucleotide targets (75%) accounted for <5% of the total cRNA expression intensity, and 1% (mostly zeins) accounted for 60% of the endosperm transcript abundance. These data closely reflect the mRNA concentrations expected for developing endosperm tissue (Woo et al., 2001). Furthermore, the expression intensities (given in normalized expression units) of each gene are a reflection of their relative RNA concentrations, although the caveats stated above regarding allelic variation and multigene families must be considered.

The data obtained from the GeneChip hybridizations showed a high degree of reproducibility, as illustrated by the comparison of transcripts from kernels of two 22-DAP ears of W64A+. Even with ears harvested from different locations and during different seasons, the results were highly reproducible, provided the endosperm samples were of a similar developmental stage and of the same genetic background. By comparison, samples from different genetic backgrounds were different to a surprising degree, in some instances surpassing the variation in transcript levels in samples from the wild type and the nearly isogenic mutant lines. This finding illustrates the importance of using nearly isogenic lines to compare patterns of gene expression between mutants.

Surprisingly, the different opaque mutations had a greater impact on gene expression in 18-DAP W64A+ endosperm than *su1*, even though this starch mutant has a striking effect on carbohydrate accumulation by 18 DAP (Doehlert and Kuo, 1994; Singletary et al., 1997). It is possible that pronounced changes in gene expression in *su1* occur at later stages of kernel development. However, an independent GeneChip profiling study of five different starch biosynthetic mutants, including *su1*, in the Oh43 background at 26 DAP also revealed a smaller degree of gene expression changes than was observed in our study of the opaque mutants (G.W. Singletary, unpublished data). Thus, it appears that, as a group, the opaque mutations have a much more pleiotropic effect on gene expression than do mutations that affect starch synthesis.

Although the opaque mutations used in this study influence the expression of a large number of genes in 18-DAP endosperm, the degree of the pleiotropic effect varied among the mutants. *o1* has the smallest effect on global patterns of gene expression (Figure 4), consistent with the relatively small differences in protein and amino acid composition in this mutant compared with the wild type (Table 1). By contrast, the large changes of protein and amino acid synthesis in *o2* (Table 1) are associated with large changes in the patterns of gene expression (Figure 3). These observations are consistent with the role of *O2* as a transcriptional activator (Schmidt et al., 1990). The O2 protein is known to regulate the expression of genes that encode the 22-kD α-zein gene family (Schmidt et al., 1992), RIP (Lohmer et al., 1991), and orthophosphate dikinase (Maddaloni et al., 1996), and our microarray analysis corroborates these observations. It also suggests that *O2* regulates a number of other genes, including 10-kD δ-zein, 15-kD β-zein, apospory-associated protein homolog (two different accessions), ARSK1 protein kinase homolog, and many others (see supplemental data online). We identified 30 genes in W64A+ that have expression levels below baseline in *o2*, and it is possible that these genes are regulated by the *O2* transcription factor. In *o2*, there is a large cumulative reduction in gene expression (49,000 expression intensity units) as a consequence of the downregulation of zein genes. However, the expression of 131 genes that were below the level of detection in W64A+ was significantly increased in *o2*. Among these are a large number of genes associated functionally with stress, cellular perturbation, and pathogen responses (Table 3). This major shift in expression from zein to nonzein genes (Table 1) is consistent with changes in patterns of protein synthesis in the endosperm that were described previously in this mutant (Damerval and De Vienne, 1993; Habben et al., 1993; Damerval and Le Guilloux, 1998).

We reported previously that the synthesis of eEF1A is increased at least twofold in W64A *o2*, and the increased accumulation of this protein is highly correlated with the Lys content of the endosperm (Habben et al., 1995; Sun et al., 1997). The GeneChip hybridization data showed that transcripts encoding eEF1A are below detectable levels in this mutant. To exclude the possibility of error that might occur as a result of hybridization with the mismatched set of probes (see above), we visually inspected the array and observed no significant hybridization to the mismatched

eEF1A sequences. Therefore, the observed downregulation of this gene in W64A *o2* most likely reflects selection of an allele for the GeneChip that is not highly expressed in this mutant. eEF1A is encoded by ~15 genes in maize, and these are expressed differentially in various tissues (Carneiro et al., 1999). Understanding the basis for the differences in eEF1A gene expression reported here and in other experiments (Habben et al., 1995; Carneiro et al., 1999) will require an Affymetrix array containing all of the maize genes that encode eEF1A.

The *fl2* mutation is the consequence of a defective signal peptide on a 22-kD α-zein protein (Coleman et al., 1997b). The failure to cleave this sequence leads to the unfolded protein response, which is manifested by a dramatic increase in ER-resident molecular chaperones (Boston et al., 1991). The effect of *fl2* on chaperone gene expression, as well as the expression of a number of stress response genes, is documented clearly by the results from the GeneChip hybridization analysis. Among the opaque mutants examined here, this pattern of gene expression is matched most closely by *Mc*, which also shows evidence of the unfolded protein response phenotype by having significant increases in the expression of ER-resident chaperones and a similar set of stress response genes. The changes we observed in the amount and size of the 16-kD γ-zein proteins in *Mc*, in conjunction with the observation of abnormally formed protein bodies in this mutant (Zhang and Boston, 1992), provide support for the hypothesis that *Mc*, like *fl2*, is related to a perturbation of zein protein deposition in protein bodies.

One group of genes consistently affected in all of the opaque mutants has been implicated routinely in stress responses, and it includes genes that encode molecular chaperones, cell wall proteins, and wound- and pathogen-activated proteins (Hammond-Kosack and Jones, 1996). The upregulation of these genes is a strong indicator of the deleterious nature of the opaque mutations and their perturbation of endosperm cell function. The penetrance of this phenotype in *o2* mutants can vary, depending on the genetic background. This is well documented in the case of the so-called "modified" *o2* maize genotypes, which develop a vitreous kernel phenotype (Vasal, 1994). The vitreous phenotype of modified *o2* mutants is controlled by several independent loci (*o2* modifiers), and their mechanism of action is not understood (Lopes et al., 1995). However, our preliminary data from experiments comparing *o2* and modified *o2* endosperm show a general reduction in the stress response of gene expression (data not shown). It is possible that an intervention in the stress response pathway constitutes the basis of *o2* modifier gene activity. It remains to be determined whether or not the phenotype of the other opaque mutants can be ameliorated by these genes.

The opaque appearance of maize kernels results from their failure to transmit light. It is assumed generally that opacity is a consequence of storage protein distribution, structure, or accumulation. However, opacity could result from any change of mature endosperm organization that increases light scattering. Conceivably, opacity could be a consequence of phenomena as distinct as a change in a developmental "switch" that influences physiological maturity and disruption in the ability of starch grains to form regular arrays as a consequence of alterations in their size, shape, or chemistry. Our data call into question the assumption involving the role of storage proteins and raise a fundamental question regarding the origin of the opaque phenotype.

Although seed protein profiles appeared unchanged in some opaque mutants (Figure 1), alteration in the abundance of at least one zein transcript in each mutant (Table 3) prevents us from excluding the hypothesis that opacity is a consequence at least in part of an alteration in protein body constitution. However, our data are consistent with at least two likely and testable alternative models. The *su1* mutant, which also has a distinct phenotype at maturity but maintains a vitreous endosperm, shows neither significant changes in gene expression nor alterations in zein transcript abundance (Table 3). However, all of the opaque mutants show a dramatic departure from the wild-type gene expression phenotype, making it reasonable to propose that this shared trait is responsible for opacity. Indeed, as in the zein RNAs, at least some stress response transcripts are altered in all of the opaque mutants. Thus, the hypotheses that an increased stress response or altered zein levels cause the opaque phenotype are equally parsimonious explanations. By contrast, despite the fact that both the *o2* and *fl2* mutations have direct effects on zein accumulation or structure, they have dissimilar effects on gene expression. Meanwhile, *o5*, *o9*, and *o11* have very similar effects on gene expression, but as a group they are equally dissimilar to *o2*, the wild type, and *fl2*. Together, these data suggest that multiple mechanisms lead to opacity, with differing effects on the pattern of gene expression in the endosperm. If this is so, the shared aspects of the gene expression pattern could be explained as the consequences of producing a "misorganized" endosperm structure.

Along with the gene expression analysis presented in this work, classic genetic experiments could be used to test these hypotheses. If the mechanisms by which the *o5*, *o9*, and *o11* mutations disrupt light transmission are related, we predict that these mutant alleles would exhibit epistatic interactions. Furthermore, suppressors of other opaque mutants, such as the *o2* modifiers (Lopes et al., 1995), should not affect *o5*, *o9*, and *o11*. Double mutants of *o5*, *o9*, and *o11* with opaque mutants outside of this phenotypically correlated cluster should be additive. However, if the basis of the mutant phenotype is zein misexpression or some other shared alteration in gene expression, such as an increased stress response, *o2* modifiers also should modify the *o5*, *o9*, *o11*, and *fl2* phenotypes and epistatic interactions would occur both within and between the phenotypically clustered mutant alleles.

The mRNA transcript profiling experiments of opaque mu-

tants with the Affymetrix GeneChip suggest the strengths as well as the weaknesses of using gene arrays to compare patterns of gene expression. Although these experiments may not identify the genetic basis of a mutant, they provide a list of genes (some with deduced functions) that are clearly affected (or not) by the mutation, and they allow us to recognize and, to a certain degree, quantify complex (pleiotropic) changes in gene expression. This is important and potentially valuable information. Unfortunately, in many cases, our knowledge of the role played by these genes is limited. Besides our ignorance of gene functions, understanding the implications of changes in the patterns of gene expression is confounded by the fact that transcript concentration is only one aspect of gene expression. Furthermore, transcript levels of a mutated allele are not necessarily affected in the mutant. This is demonstrated in our study, for instance, by the levels of the *fl2* and *su1* transcripts in their respective mutant endosperms. Nevertheless, the concentration of the *o2* transcript in W64A *o2* endosperm is diminished greatly. Another limitation of gene microarray data is the closed nature of the experiments, which are limited to the predetermined set of genes. "Open" technologies for mRNA transcript profiling, such as Serial Analysis of Gene Expression-related techniques (Shimkets et al., 1999), address these limitations by providing the opportunity to analyze all of the expressed genes, regardless of whether they have been isolated. We are using these approaches at present to further dissect the pleiotropic effects of the maize opaque endosperm mutations.

METHODS

Maize Mutants

o2 and *fl2* inbred lines of W64A maize (*Zea mays*) were obtained from C.Y. Tsai (Purdue University, West Lafayette, IN) and were maintained at the University of Arizona (Tucson) since 1988. The *su1* mutant in the W64A background, and the *o1*, *o5*, *o9*, and *o11* mutants in different germplasm backgrounds, were obtained from the Maize Genetics Stock Center at the University of Illinois (Champaign-Urbana). The *DeB30* and *Mc* mutants were provided by Francesco Salamini (Instituo Sperimentale per la Cerealicoltura, Bergamo, Italy). The *o1*, *o5*, *o9*, *o11*, *Mc*, and *DeB30* mutants were converted to the W64A background by backcrossing six times, followed by two self-pollinations. Plants used for the protein analysis were grown at the University of Arizona Campus Agricultural Center in 1998.

SDS-PAGE and Immunoblot Analysis

Endosperm flour was prepared by the methods of Wang and Larkins (2001). After pooling flour from 15 kernels, the protein in 50-mg aliquots was separated into zein and nonzein proteins and analyzed by SDS-PAGE, as described by Habben et al. (1993). Polyacrylamide gels were either stained with Coomassie Brilliant Blue R250 or blotted onto nitrocellulose using either a Trans-Blot Semi-Dry Transfer Cell or the Mini-Trans-Blot Cell (Bio-Rad, Hercules, CA). Zeins and other seed proteins were immunodetected (Harlow and Lane, 1988) with monospecific rabbit antisera that react with total α-zeins (1:5000 dilution), the 19-kD B α-zein and D α-zein proteins (1:10,000), the 22-kD α-zeins (1:10,000), the 50-kD (1:10,000), 27-kD (1:10,000), and 16-kD γ-zein proteins (1:5000), the 15-kD β-zein (1:5000), the 18- and 10-kD δ-zeins (1:5000), 18-kD α-globulin (1:3000), legumin1 (1:3000), and legumin2 (1:5000). Antiserum reacting with maize legumin2 was developed with a bacterially expressed His tag fusion (Harlow and Lane, 1988) of the entire legumin2 coding sequence. The antibody against the 18-kD δ-zein was developed with a bacterially expressed His tag fusion of a partial 18-kD δ-zein polypeptide (nucleotides 71 to 125). This 18-kD δ-zein antibody also cross-reacts weakly with 10-kD δ-zein polypeptides. All other antisera were as described previously (Woo et al., 2001). The total α-zein antiserum was described by Lending et al. (1988).

Protein and Amino Acid Analyses

Protein analyses were performed with endosperm flour from mature kernels as described previously (Moro et al., 1995). Amino acid analysis (after performic acid oxidation) was performed at the protein analytical facility of the University of Iowa (Iowa City). Measurements were made with pooled samples of 15 kernels of each genotype, and the data presented are the means of two independent assays.

RNA Preparation and Hybridization

The maize inbred lines Oh43+, W64A+, and the W64A nearly isogenic mutant lines of *su1*, *o1*, *o2*, *o5*, *o9*, *o11*, *Mc*, and *fl2* were grown in the summer of 1998 in adjacent field plots at the Pioneer Hi-Bred International genetic nursery in Johnston, IA. Plants were hand pollinated, and a minimum of six well-filled ears of each line were harvested 18 days after pollination (22 days after pollination in one case) and frozen immediately in liquid nitrogen. Kernels were taken from the center of each ear, and the endosperm was dissected from the embryo and pericarp. To minimize the effect of biological variation between ears on gene expression, equal numbers of dissected endosperms from three ears were pooled and treated as one sample; thus, a minimum of two replicated samples was used for each experiment. To compare ear-to-ear variation, an analysis was done with two W64A+ ears harvested at 22 days after pollination.

Total RNA was prepared from frozen, ground endosperm tissue using the Trizol reagent (Gibco BRL, Gaithersburg, MD) according to the manufacturer's suggested protocol. Poly(A)$^+$ RNA was isolated using the PolyA Tract mRNA Isolation kit IV (Promega, Madison, WI), and double-stranded cDNA was synthesized using the SuperScript Choice System (Gibco BRL). Copy RNA probes were synthesized subsequently with biotin-conjugated CTP and UTP ribonucleotides (MEGAscript T7 kit; Ambion, Austin, TX) and purified with RNeasy (Qiagen, Valencia, CA). Amplified copy RNA (12 μg) was fragmented, combined with nonplant controls, and hybridized to the GeneChip arrays according to Affymetrix (Santa Clara, CA) protocols. The hybridized microarrays were washed and stained with a streptavidin R-phycoerythrin conjugate (Affymetrix Fluidics Station) and then scanned with a Hewlett-Packard Gene Array Scanner (Palo Alto, CA).

Each image was inspected visually for hybridization artifacts and manufacturing defects.

Maize GeneChip Design and Data Analysis

The maize GeneChip microarrays manufactured by Affymetrix contained 64,324 oligodeoxynucleotides derived from maize cDNA sequences. A table of 1442 genes is presented in the supplemental data online. The cDNA sequences represented a selection of various maize genes that are expressed differentially or ubiquitously. Most of these genes have assigned or hypothetical functions based on homology with known genes. Approximately 200 genes had no recognized function as of January 2002. Twenty oligodeoxyribonucleotide pairs, consisting of overlapping match and mismatch probes (20 nucleotides long), were synthesized for each gene. A small number of genes were represented by <20 oligodeoxyribonucleotide pairs. However, these sequence sets generated inconsistent results, and the corresponding data are not reported. The specific design of the oligodeoxyribonucleotide sequences used is a trade secret of Affymetrix and was not available for our evaluation.

Affymetrix GeneChip Analysis Suite 3.0 was used to evaluate the hybridization signals and determine the average difference values (expression intensities) between perfectly matched oligodeoxyribonucleotide probes and the 1-bp mismatches for each probe set. To compare gene expression in W64A+ and the mutant genotypes, it was necessary to standardize the expression data. Because of the pleiotropic effects of the opaque mutants on gene expression, the data sets obtained in this study were refractory to the data-scaling procedures recommended by Affymetrix (http://www.affymetrix.com/products/is.html) (Wodicka et al., 1997). Instead, the fluorescence intensity data, presented as arbitrary "expression" units, were scaled globally using W64A+ as the reference, as described below. Arbitrary expression data from each of the experiments were organized into spreadsheets on Excel (Microsoft, Redmond, WA). All calculations and manipulations then were performed within Excel.

First, data from the two independent replications of each genotype were compared with each other by standard linear regression, and a regression coefficient was calculated. This regression coefficient (slope) was used as a scaling factor to normalize replicate data sets to each other, and the two normalized data sets were averaged. Second, each of the averaged mutant (treatment) data sets was scaled to the averaged W64A+ (control) data set using a two-step regression analysis. The first step identified 2% of the genes among the mutant and reference sets with the most outlying data points. These genes were omitted before the second step of the analysis, and the regression coefficient obtained from the second comparison was used as a scaling factor to normalize the average expression units for each measured gene to that in W64A+. Finally, after these scaling steps were performed, relative intensity data with a numeric value <20, including negative values, were considered not detected and, according to Affymetrix conventions, systematically set to a baseline of 20 arbitrary expression units. A "trimmed" mean is more appropriate to this situation, in which there are outliers, such as zeins, that unduly influence the mean. This scaling procedure more appropriately considers the distribution of these data sets (Wonnacott and Wonnacott, 1990). The globally scaled, normalized values are presented in the supplemental data online and reflect the abundance of a particular gene relative to the total mRNA populations. These values permitted a more conservative, direct comparison of all data points, regardless of the experiment from which they originated. By contrast, most notably with the W64A *o2* data set, the normalization method recommended by Wodicka et al. (1997) resulted in scaling the data such that the majority of the "treatment" expression units appeared different from the expression units of the "control."

Materials Distribution Statement

Novel materials described in this article will be made available for noncommercial research purposes upon acceptance and signing of a material transfer agreement. In some cases, such materials may contain or be derived from materials obtained from a third party. In such cases, distribution of material will be subject to the requisite permission from any third-party owners, licensors, or controllers of all or parts of the material. Obtaining any permission will be the sole responsibility of the requester.

Accession Numbers

The accession numbers for legumin1 and legumin2 are AF372987 and AF372988, respectively.

ACKNOWLEDGMENTS

We are grateful to our colleagues who made critical suggestions to improve the manuscript, in particular David Galbraith at the University of Arizona. We are indebted to Paul Anderson and Larry Beach at Pioneer Hi-Bred International, who encouraged this work. We thank Virginia Dress and David Hu for technical support and Sean Yang and Carol Hendrick for bioinformatics support. We further thank colleagues in the Pioneer Hi-Bred Analytical Biochemistry Department and the Dupont-Pioneer genomics groups for their expert support. A special thanks to Jeff Kraft for assistance with the immunoblots and figure preparation. This research was supported by grants from the Department of Energy (DE-FG03-96ER20242) and Pioneer Hi-Bred International to B.A.L.

Received April 16, 2002; accepted July 18, 2002.

REFERENCES

Balconi, C., Berardo, N., Reali, A., and Motto, M. (1998). Variation in protein fractions and nitrogen metabolism of developing normal and opaque endosperm mutants of maize. Maydica **43,** 195–203.

Boston, R.S., Fontes, E.B., Shank, B.B., and Wrobel, R.L. (1991). Increased expression of the maize immunoglobulin binding protein homolog b-70 in three zein regulatory mutants. Plant Cell **3,** 497–505.

Carneiro, N., Hughes, P., and Larkins, B.A. (1999). The eEFlA gene family is differentially expressed in maize endosperm. Plant Mol. Biol. **41,** 801–813.

Chandrashekar, A., and Mazhar, H. (1999). The biochemical basis

and implications of grain strength in sorghum and maize. J. Cereal Sci. **30,** 193–207.

Coleman, C., Dannenhoffer, J., and Larkins, B.A. (1997a). The prolamin proteins of maize, sorghum and coix. In Advances in Cellular and Molecular Biology of Plants, B.A. Larkins and I.K. Vasil, eds (Dordrecht, The Netherlands: Kluwer Academic Publishers), pp. 257–288.

Coleman, C., and Larkins, B.A. (1999). The prolamins of maize. In Seed Proteins, P.R. Shewry and R. Casey, eds (Dordrecht, The Netherlands: Kluwer Academic Publisher), pp. 109–139.

Coleman, C.E., Clore, A.M., Ranch, J.P., Higgins, R., Lopes, M.A., and Larkins, B.A. (1997b). Expression of a mutant alpha-zein creates the floury2 phenotype in transgenic maize. Proc. Natl. Acad. Sci. USA **94,** 7094–7097.

Damerval, C., and De Vienne, D. (1993). Quantification of dominance for proteins pleiotropically affected by opaque-2 in maize. Heredity **70,** 38–51.

Damerval, C., and Le Guilloux, M. (1998). Characterization of novel proteins affected by the o2 mutation and expressed during maize endosperm development. Mol. Gen. Genet. **257,** 354–361.

Dannenhoffer, J.M., Bostwick, D.E., Or, E., and Larkins, B.A. (1995). opaque-15, a maize mutation with properties of a defective opaque-2 modifier. Proc. Natl. Acad. Sci. USA **92,** 1931–1935.

Doehlert, D.C., and Kuo, T.M. (1994). Gene expression in developing kernels of some endosperm mutants of maize. Plant Cell Physiol. **35,** 411–418.

Eisen, M.B., Spellman, P.T., Brown, P.O., and Botstein, D. (1998). Cluster analysis and display of genome-wide expression patterns. Proc. Natl. Acad. Sci. USA **95,** 14863–14868.

Fontes, E.B.P., Shank, B.B., Wrobel, R.L., Mosse, S.P., O'Brian, G.R., Wurtzel, E.T., and Boston, R.S. (1991). Characterization of an immunoglobulin binding protein homolog in the maize *floury*-2 endosperm mutant. Plant Cell **3,** 483–496.

Geetha, K.B., Lending, C.R., Lopes, M.A., Wallace, J.C., and Larkins, B.A. (1991). opaque-2 modifiers increase gamma-zein synthesis and alter its spatial distribution in maize endosperm. Plant Cell **3,** 1207–1219.

Gillikin, J.W., Zhang, F., Coleman, C.E., Bass, H.W., Larkins, B.A., and Boston, R.S. (1997). A defective signal peptide tethers the floury-2 zein to the endoplasmic reticulum membrane. Plant Physiol. **114,** 345–352.

Giroux, M.J., Boyer, C., Feix, G., and Hannah, L.C. (1994). Coordinated transcriptional regulation of storage product genes in the maize endosperm. Plant Physiol. **106,** 713–722.

Habben, J.E., Kirleis, A.W., and Larkins, B.A. (1993). The origin of lysine-containing proteins in opaque-2 maize endosperm. Plant Mol. Biol. **23,** 825–838.

Habben, J.E., Moro, G.L., Hunter, B.G., Hamaker, B.R., and Larkins, B.A. (1995). Elongation factor 1 alpha concentration is highly correlated with the lysine content of maize endosperm. Proc. Natl. Acad. Sci. USA **92,** 8640–8644.

Hammond-Kosack, K.E., and Jones, J.D.G. (1996). Resistance gene-dependent plant defense responses. Plant Cell **8,** 1773–1791.

Harlow, E., and Lane, D. (1988). Antibodies: A Laboratory Manual. (Cold Spring Harbor, NY: Cold Spring Harbor Laboratory Press).

James, M.G., Robertson, D.S., and Myers, A.M. (1995). Characterization of the maize gene sugary1, a determinant of starch composition in kernels. Plant Cell **7,** 417–429.

Kirleis, A.W., and Stroshine, R. (1990). Effects of hardness and drying air temperature on breakage susceptibility and dry-milling characteristics of yellow dent corn. Cereal Chem. **67,** 523–528.

Knight, J. (2001). When the chips are down. Nature **410,** 860–861.

Kodrzycki, R., Boston, R.S., and Larkins, B.A. (1989). The opaque-2 mutation of maize differentially reduces zein gene transcription. Plant Cell **1,** 105–114.

Larkins, B.A., and Hurkman, W.J. (1978). Synthesis and deposition of zein in protein bodies of maize endosperm. Plant Physiol. **62,** 256–263.

Lee, K.H., Jones, R.A., Dalby, A., and Tsai, C.Y. (1976). Genetic regulation of storage protein content in maize endosperm. Biochem. Genet. **14,** 641–649.

Lending, C.R., and Larkins, B.A. (1989). Changes in the zein composition of protein bodies during maize endosperm development. Plant Cell **1,** 1011–1023.

Lending, C.R., Kriz, A., Larkins, B.A., and Bracker, C. (1988). Structure of maize protein bodies and immunocytochemical localization of zeins. Protoplasma **143,** 51–62.

Lohmer, S., Maddaloni, M., Motto, M., Di Fonzo, N., Hartings, H., Salamini, F., and Thompson, R.D. (1991). The maize regulatory locus Opaque-2 encodes a DNA-binding protein which activates the transcription of the b-32 gene. EMBO J. **10,** 617–624.

Lopes, M.A., Coleman, C.E., Kodrzycki, R., Lending, C.R., and Larkins, B.A. (1994). Synthesis of an unusual alpha-zein protein is correlated with the phenotypic effects of the floury2 mutation in maize. Mol. Gen. Genet. **245,** 537–547.

Lopes, M.A., Takasaki, K., Bostwick, D.E., Helentjaris, T., and Larkins, B.A. (1995). Identification of two opaque2 modifier loci in quality protein maize. Mol. Gen. Genet. **247,** 603–613.

Lyznik, L.A., and Tsai, C.Y. (1989). Protein synthesis in endosperm cell cultures of maize (*Zea mays* L.). Plant Sci. **63,** 105–114.

Maddaloni, M., Donini, G., Balconi, C., Rizzi, E., Gallusci, P., Forlani, F., Lohmer, S., Thompson, R., Salamini, F., and Motto, M. (1996). The transcriptional activator Opaque-2 controls the expression of a cytosolic form of pyruvate orthophosphate dikinase-1 in maize endosperms. Mol. Gen. Genet. **250,** 647–654.

Marks, M.D., Lindell, J.S., and Larkins, B.A. (1985). Nucleotide sequence analysis of zein mRNAs from maize endosperm. J. Biol. Chem. **260,** 16451–16459.

Mestres, C., and Matencio, F. (1996). Biochemical basis of kernel milling characteristics and endosperm vitreousness of maize. J. Cereal Sci. **24,** 283–290.

Moro, G.L., Lopes, M.A., Habben, J.E., Hamaker, B.R., and Larkins, B.A. (1995). Phenotypic effects of opaque2 modifier genes in normal maize endosperm. Cereal Chem. **72,** 94–99.

Nelson, O.E., Mertz, E.T., and Bates, L.S. (1965). Second mutant gene affecting the amino acid pattern of maize endosperm proteins. Science **150,** 1469–1470.

Neuffer, M.G., Coe, E., and Wessler, S. (1997). Mutants of Maize. (Cold Spring Harbor, NY: Cold Spring Harbor Laboratory Press).

Schmidt, R.J., Burr, F.A., Aukerman, M.J., and Burr, B. (1990). Maize regulatory gene opaque-2 encodes a protein with a "leucine-zipper" motif that binds to zein DNA. Proc. Natl. Acad. Sci. USA **87,** 46–50.

Schmidt, R.J., Ketudat, M., Aukerman, M.J., and Hoschek, G. (1992). Opaque-2 is a transcriptional activator that recognizes a specific target site in 22-kD zein genes. Plant Cell **4,** 689–700.

Shank, K.J., Su, P., Brglez, I., Boss, W.F., Dewey, R.E., and Boston, R.S. (2001). Induction of lipid metabolic enzymes during the endoplasmic reticulum stress response in plants. Plant Physiol. **126,** 267–277.

Shimkets, R.A., et al. (1999). Gene expression analysis by transcript profiling coupled to a gene database query. Nat. Biotechnol. **41,** 801–813.

Singletary, G.W., Banisadr, R., and Keeling, P.L. (1997). Influence of gene dosage on carbohydrate synthesis and enzymatic activities in endosperm of starch-deficient mutants of maize. Plant Physiol. **113,** 293–304.

Sun, Y.M., Carneiro, N., Clore, A.M., Moro, G.L., Habben, J., and Larkins, B.A. (1997). Characterization of maize elongation factor 1A and its relationship to protein quality in the endosperm. Plant Physiol. **115,** 1101–1107.

Swarup, S., Timmermans, M.C., Chaudhuri, S., and Messing, J. (1995). Determinants of the high-methionine trait in wild and exotic germplasm may have escaped selection during early cultivation of maize. Plant J. **8,** 359–368.

Thompson, G., and Larkins, B.A. (1994). Characterization of zein genes and their regulation in maize endosperms. In The Maize Handbook, M. Freeling and V. Walbot, eds (Berlin: Springer-Verlag), pp. 639–646.

Tsai, C.Y., Huber, D.M., and Warren, H.L. (1978). Relationship of the kernel sink for N to maize productivity. Crop Sci. **18,** 399–404.

Vasal, S.K. (1994). High quality protein corn. In Specialty Corns, A.R. Hallauer, ed (Boca Raton, FL: CRC Press), pp. 79–121.

Wallace, J.C., Lopes, M.A., Paiva, E., and Larkins, B.A. (1990). New methods for extraction and quantitation of zeins reveal a high content of gamma-zein in modified opaque-2 maize. Plant Physiol. **92,** 191–196.

Wang, X., and Larkins, B.A. (2001). Genetic analysis of amino acid accumulation in opaque-2 maize endosperm. Plant Physiol. **125,** 1766–1777.

Wodicka, L., Dong, H., Mittmann, M., Ho, M.H., and Lockhart, D.J. (1997). Genome-wide expression monitoring in *Saccharomyces cerevisiae*. Nat. Biotechnol. **15,** 1359–1367.

Wonnacott, T.H., and Wonnacott, R.J. (1990). Introductory Statistics. (New York: John Wiley & Sons), pp. 536–539.

Woo, Y.-M., Hu, D.W.-N., Larkins, B.A., and Jung, R. (2001). Genomics analysis of genes expressed in maize endosperm identifies novel seed proteins and clarifies patterns of zein gene expression. Plant Cell **13,** 2297–2317.

Zhang, F., and Boston, R.S. (1992). Increases in binding protein (BiP) accompany changes in protein body morphology in 3 high-lysine mutants of maize. Protoplasma **171,** 142–152.